Supporting Information

Assessing the functional selectivity of an arsenic sensing protein *in vitro* and *in vivo*

Annamária Tóth,[a] Bálint Hajdu,[a,b] Zeyad H. Nafaee,[a,c] Réka Sára Gyimesi,[a] Béla Gyurcsik,[a] Éva Hunyadi-Gulyás,[d] Joao Guilherme Correia,[e,f] Juliana Schell,[e,g] Thanh Thien Dang,[g] Kohsuke Kato,[h] Atsushi Kawaguchi,[h] Lars Hemmingsen[b] and Attila Jancsó*[a]

[a] *Department of Molecular and Analytical Chemistry, University of Szeged, Dóm tér 7-8. H-6720 Szeged, Hungary;* [b] *Department of Chemistry, University of Copenhagen, Universitetsparken 5, 2100 København Ø, Denmark* [c] *College of Pharmacy, University of Babylon, Hillah 51001, Iraq;* [d] *Proteomics Research Group, Core Facility, Biological Research Centre, HUN-REN, Temesvári krt. 62, H-6726, Szeged, Hungary;* [e] *European Organization for Nuclear Research (CERN), CH-1211 Geneva, Switzerland;* [f] *Centro de Cięncias e Tecnologias Nucleares, Departamento de Engenharia e Cięncias Nucleares, Instituto Superior Técnico, Universidade de Lisboa, 2695-066 Bobadela LRS, Portugal;* [g] *Institute for Materials Science and Center for Nanointegration Duisburg-Essen (CENIDE), University of Duisburg-Essen, 45141 Essen, Germany;* [h] *Department of Infection Biology, Institute of Medicine, University of Tsukuba, 1-1-1 Tennodai, Tsukuba, 305-8575, Japan;*

Table of Contents

Experimental Procedures

Materials

Anhydrous arsenic(III) oxide, potassium antimonyl tartrate trihydrate, mercury(II) chloride, lead(II) chloride, zinc(II) perchlorate hexahydrate, sodium perchlorate, ammonium bicarbonate, dithiothreitol (DTT), meso-2,3-Dimercaptosuccinic acid, imidazole, phenylalanine, cetyltrimethylammonium bromide (CTAB) and perfluoropentanoic acid (PFPA) were purchased from Merck (Sigma-Aldrich), sodium chloride, potassium chloride, sodium dihydrogen phosphate, disodium hydrogen phoshate, tris(hydroxymethyl)aminomethane (TRIS), 2-(N-morpholino)ethanesulfonic acid (MES), 2-(Cyclohexylamino)ethanesulfonic acid (CHES), glucose and glycine from Molar Chemicals, and acrylamide/bisacrylamide (29/1) 30% (w/v) solution from SERVA Electrophoresis GmbH. Cadmium(II) perchlorate hexahydrate, L-arabinose, ortho-nitrophenyl-β-galactoside (ONPG), 5-bromo-4-chloro-3-indolyl-β-D-galactopyranoside (X-gal), sodium deoxycholate and tris(2-carboxyethyl)phosphine hydrochloride (TCEP) was a product of Thermo Scientific Chemicals and the Lysogeny Broth (LB) medium and LB-agar powders were from REANAL Laborvegyszer KFT. Both ampicillin sodium salt and kanamycin sulfate were derived from Serva. All chemicals were used without further purification. Metal ion and metalloid stock solutions were prepared by weighing out calculated amounts of their compounds and dissolution of the solids in MilliQ water, with the exception of arsenous(III) oxide which was dissolved in 0.1 M NaOH and then neutralized by a 0.1 M $HClO_4$ solution. The exact concentrations of these solutions were calculated based on the accurate masses of the pure, stoichiometric solid compounds, or by performing complexometric titrations with and EDTA titrant, as described in our previous work.[1] The arsenous acid, antimonyl tartrate, lead(II) chloride and mercury(II) chloride solutions were prepared by weighing calculated masses of the relevant compounds – arsenous oxide (As_2O_3), potassium antimonyl tartrate trihydrate ($C_8H_4K_2O_{12}Sb_2{\cdot}3H_2O$), lead(II) chloride ($PbCl_2$) and mercury(II) chloride ($HgCl_2$), respectively – into volumetric flasks and after dissolution, their concentrations were calculated based on the known molecular masses of the highly pure, stoichiometric, commercial compounds. Concentrations of the cadmium(II) chloride and zinc(II) chloride stock solutions were determined by complexometric titration.[2] The preciese concentration of the ~0.05 M EDTA solution was determined by titrating $Pb(NO_3)_2$ standard samples at pH ~ 6.0 (hexamethylenetetramine/nitric acid buffer) using methyl thymol blue indicator. Concentrations of the zinc(II) chloride and cadmium(II) perchlorate stock solutions were determined using the standardized EDTA solution under the same conditions (pH ~ 6.0, hexamethylenetetramine/nitric acid buffer) using methyl thymol blue and xylenol orange indicators, respectively. The pH of the various buffer solutions, used for the purification and storage of the protein or for the preparation of samples for different experiments, was adjusted by sodium hydroxide and/or hydrochloric acid solutions and by using a Metrohm 6.0234.100 combined pH glass electrode connected to an Orion 710A digital pH-meter, calibrated at room temperature (T = 298 K) with standard buffer solutions.

(Caution: Solid arsenic(III) oxide is a chemical with high health hazards (acute toxicity, skin corrosion, serious eye damage, and carcinogenicity) and environmental hazards (long-term (chronic) aquatic hazard) and should be handled with extreme care using the necessary protective equipment. Other metal salts used in this study also pose serious health hazards. Potassium antimonyl tartrate trihydrate: acute oral toxicity, acute inhalation toxicity, specific target organ toxicity (single exposure). Lead-chloride: acute toxicity, reproductive toxicity, hazardous to the aquatic environment (acute and chronic hazard). Mercury chloride: acute toxicity (oral), acute toxicity (dermal), reproductive toxicity, skin corrosion, hazardous to the aquatic environment (acute and chronic hazard). Cadmium perchlorate: acute toxicity (oral), acute toxicity (dermal), acute inhalation toxicity. Any solution samples containing the aqueous forms of arsenic(III), antimony(III), mercury(II), lead(II) and cadmium(II) are also toxic and must be handled/disposed according to the regulations for toxic liquid wastes.)

Plasmid constructions

The pdUA-$LacI_{NE}$-AfArsR plasmid, including the recognition site of AfArsR was constructed for use in intracellular assays (see below) to regulate the expression of the *lacI* gene through AfArsR binding or release. Thus, the 5'-ctagCATCCACGAATATTTCTTGCAGTATTGACAAGATATCG-3' and the 5'-

aattCGATATCTTGTCAATACTGCAAGAAATATTCGTGGATG-3’ deoxy-oligonucleotides (Fasmac) were hybridized by 1 °C/min cooling rate from 95 °C to 10 °C in 100 µM final concentration in the presence of 10 mM $NaClO_4$. The resulting double strand DNA had the appropriate sticky ends compatible with the 5’-G▼CTAGC-3’ cleavage pattern of the NheI and 5’-G▼AATTC-3’ cleavage pattern of EcoRI restriction endonucleases. The digestion of the pdUA-$lacI_{NE}$ vector (kindly provided by Dr. Antal Kiss, Institute of Biochemistry, HUN-REN Biological Research Centre, Hungary) was performed by 0.4 U/µl NheI and EcoRI restriction enzymes (TOYOBO) at 37 °C for 2 h in 1 × M Buffer (Toyobo). The digestion was terminated at 65 °C for 20 min. The digestion product was purified by extraction with phenol/chloroform mixture and then the DNA was precipitated by ethanol. The ligation of ~ 100 ng plasmid DNA with hybridized DNA (applied at ~ 10× molar excess) was carried out using equal volume of the Ligation High Ver.2 master mix (TOYOBO) at 16 °C for 30 minutes. *E. coli* DH5α competent cells were transformed with the ligation mixture, then plated and cultured in 5 ml LB medium containing 0.05 mg/ml kanamycin in order to amplify the plasmid DNA. The gene of *Acidithiobacillus ferrooxidans* ArsR (AfArsR) was kindly provided by prof. Saravanamuthu Thiyagarajan (Institute of Bioinformatics and Applied Biotechnology, Bengaluru, Karnataka 560100, India)[3] inserted in a pBAD/myc-His-C (Amp^R)[4] vector designated as pBAD-AfArsR. The full coding sequence included in this plasmid is:

ATGGAACCACTACAAGACCCTGCACAAATCGTCGCCCGCCTGGAGGCCCTGGCCTCGCCGGTGCGCCTGGAGATTTTTC
GCCTGCTGGTAGAACAGGAGCCGACGGGTCTGGTATCCGGCGATATTGCCGAGCATCTGGGGCAACCGCACAACGGCA
TTTCCTTTCATCTGAAAAACCTCCAGCACGCCGGGCTGGTCACCGTGCAGCGCGAAGGACGCTATCAGCGTTACCGGGCA
GCCATGCCCGTGGTGCGCGCGCTGGTCGCGTATCTCACAGAAAATTGCTGCCACGGTACCCGGGACTGTGCCCTATCCG
GTGAAACCCGCTCTCCCTCAGTCCAGGAAGGAAACCAGGTCGACCATCATCATCATCATCAT**TGA**

The His-tagged AfArsR protein sequence encoded by this DNA is as follows:

MEPLQDPAQIVARLEALASPVRLEIFRLLVEQEPTGLVSGDIAEHLGQPHNGISFHLKNLQHAGLVTVQREGRYQRYRAAMPV
VRALVAYLTENCCHGTRDCALSGETRSPSVQEGNQVDHHHHHH

We have designed several mutants highlighted in the above sequences with the following color backgrounds: **R85A, C95A, C96A, C95A/C96A, H97A, H97D, R100A, D101A, C102A**

All the mutated genes were established by a Quikchange type point mutation using the designed primers listed in Table S1. For this purpose, a 32-cycle polymerase chain reaction (PCR) was carried out at 98 °C denaturing, 65-72 °C annealing (Table S1) and 72 °C extension temperature using 0.02 U/µl Phusion High-Fidelity DNA Polymerase (Thermo Scientific) in 1 × Phusion HF buffer. The PCR products were purified by extraction with phenol/chloroform mixture and by precipitation with ethanol and the pellets were dissolved in 20 µL sterilized MilliQ water. Afterwards, the 5’-termini of the purified DNA were phosphorylated using 0.5 U/µl T4 Polynucleotide Kinase (TOYOBO) in 1 × Reaction Buffer A at 37 °C for 60 minutes, terminated at 75 °C for 10 min. We ran the whole amounts of DNAs on 1 % agarose gel and the cut-out bands were purified by FastGene Gel/PCR Extraction Kit.

Table S1 List of the designed oligonucleotides for the Quikchange type point mutation of the AfArsR protein and the relevant annealing temperatures used during the PCR process.

Name	Sequence	Annealing temperature in the first 3 cycles	Annealing temperature in the last 29 cycles
C95A-QF	5’- CTGCCACGGTACCCGGGA -3’	65 °C	68.5 °C
C95A-QR	5’- gcATTTTCTGTGAGATACGCGACCAG -3’		
C96A-QF	5’- CCACGGTACCCGGGACTGT -3’	65 °C	68.5 °C
C96A-QR	5’- gcGCAATTTTCTGTGAGATACGCGA -3’		
C95,96A-QF	5’- gcCCACGGTACCCGGGACTGT -3’	68.5 °C	72 °C
C95,96A-QR	5’- GgcATTTTCTGTGAGATACGCGACCAGC -3’		
H97D-QF	5’- ACGGTACCCGGGACTGTGCC -3’	68.5 °C	72 °C
H97D-QR	5’- cGCAGCAATTTTCTGTGAGATACGCGAC -3’		

C102A-QF	5'- gcTGCCCTATCCGGTGAAACC -3'	65 °C	67.5 °C
C102A-QR	5'- GTCCCGGGTACCGTGGC -3'		
H97A-QF	5'- CGGTACCCGGGACTGTGC -3'	65 °C	67.5 °C
H97A-QR	5'- gcGCAGCAATTTTCTGTGAGATACG -3'		
R85A-QF	5'- cCGCGCTGGTCGCGTATC -3'	65 °C	67.5 °C
R85A-QR	5'- cCACCACGGGCATGGCTG -3'		
D101A-QF	5'- cCTGTGCCCTATCCGGTGAAAC -3'	65 °C	67.5 °C
D101A-QR	5'- CCCGGGTACCGTGGCAG -3'		
R100A-QF	5'- cGGACTGTGCCCTATCCGG -3'	65 °C	67.5 °C
R100A-QR	5'- cGGTACCGTGGCAGCAATTTTC -3'		

The concentration of the purified DNAs were determined by a NanoDrop Lite Spectrophotometer (Thermo Scientific). ~ 100 ng DNAs were re-circularized at room temperature for an hour using equal volume from the Ligation High Ver. 2 (TOYOBO) ligase enzyme. *E. coli* DH5α competent cells were transformed with the ligation mixture, then plated and cultured in 5 ml LB medium containing 0.1 mg/ml ampicyllin to amplify the plasmid DNA. ZR Plasmid Miniprep – Classic Kit (Zymo Research) or NucleoSpin Plasmid DNA purification kit (Macherey-Nagel) was used for small scale plasmid purification for every DNA vector carrying insert DNAs. All DNA constructs were checked by standard DNA sequencing with BigDye Terminator v3.1 Cycle Sequencing Kit on an Applied Biosystems 3500 Genetic Analyzer before further use.

Protein expression and purification

E. coli BL21 (DE3) bacteria transformed by pBAD-AfArsR were first grown in 5 ml LB medium including 0.1 mg/ml ampicillin at 37 °C with shaking until OD_{600} ~ 0.6 was reached. 500 µL portion of this bacterial culture was transferred into 250 mL LB media including 0.1 mg/ml ampicillin and these cells were grown at 37 °C. When OD_{600}~0.6 was reached, c_{final} = 2.66 mM L-arabinose was added into the pre-grown culture to induce the expression of the AfArsR protein followed by an additional 3-hour incubation at 37 °C. The cells were harvested by centrifugation at 4 °C, 4000 g for 15 minutes discarding the supernatant. The bacterial pellets were re-suspended into 20 ml 1×PBS (Phosphate Buffer Saline) + 110 mM NaCl buffer, pH = 7.3, containing in total 250 mM NaCl, 2.7 mM KCl, 10 mM Na_2HPO_4, and 1.8 mM KH_2PO_4. The cells were lysed by sonication on ice at 45% amplitude (10 × 15 s pulses) using a VCX 130 PB (130 W) ultrasonic processor equipped with a titanium probe (13 mm tip diameter). The extract was centrifuged at 4 °C and 16500 g for 30 minutes and the supernatant was further purified in two steps. First, nickel affinity chromatography was implemented using gradient elution by 0-500 mM imidazole in 1×PBS + 110 mM NaCl buffer, pH = 7.3 on an XK 16/20 column loaded with IMAC Sepharose 6 FF resin chelated with Ni(II) using an ÄKTA ¨ FPLC explorer system (Amersham Pharmacia Biotech). 5 mL fractions were collected based on the detected absorbance at 280 nm and they were run on 15 % sodium-dodecyl sulfate (SDS) polyacrylamide gel and stained by Coomassie Brilliant Blue as in our earlier work[5] and the identified protein fractions were further purified. Buffer exchange of the IMAC fractions to 20 mM TRIS-HCl, pH = 7.4, containing 200 µM DTT was carried out by ultrafiltration using an Amicon Ultra (15 mL) centrifugal filter (Merck Millipore Ltd) at 4 °C, 4000 g. Total reduction of the protein by 10 mM DTT (final concentration) for 1 hour at room temperature was performed prior the ultrafiltration step to prevent the oxidation caused aggregation of the protein on the filter. The ultrafiltered solution was then exposed to anionic exchange chromatography on a HiPrep Q Sepharose FF column (GE Healthcare/BioScience). The target protein was eluted using a gradient elution by 0-1 M NaCl in 20 mM TRIS-HCl, pH = 7.4 buffer. 5 mL fractions were collected and analysed by SDS-PAGE. The identification of AfArsR was carried out by mass spectroscopy directly from the gel as described in an earlier work.[5] Finally, after the reduction of the protein by 10 mM DTT, the buffer of the selected fractions was changed by ultrafiltration to 20 mM ammonium bicarbonate buffer, pH =7.6 with 400 µM TCEP for long term storage at –80 °C.

To compare the protein expression levels of the various mutants, we transformed *E. coli* BL21 (DE3) bacteria separately by the various pBAD/myc-His-C (Amp^R)[3] vectors containing the gene of the wild type or the different AfArsR mutant proteins (see the "*Plasmid constructions"* section above). These cell cultures were grown in 5

mL LB medium including 0.1 mg/ml ampicillin at 37 °C with shaking until OD_{600} ~ 0.6 was reached, when c_{final} = 2.66 mM L-arabinose was applied (except of the control sample) to induce the protein expression followed by an additional 2-hour incubation at 37 °C. The cells were harvested by centrifugation at 13000 rpm for 1 minutes using an Eppendorf MiniSpin Plus centrifuge discarding the supernatant. The bacterial pellets were re-suspended into 400 – 400 µl 1×PBS (Phosphate Buffer Saline) + 110 mM NaCl buffer, pH = 7.3. The cells were lysed by sonication on ice at 45% amplitude (10 × 15 s pulses) using a VCX 130 PB (130 W) ultrasonic processor equipped with a titanium probe (3 mm tip diameter). The extracts were centrifuged at room temperature and 13500 rpm for 15 minutes in an Eppendorf MiniSpin Plus centrifuge and 20 – 20 µL of the supernatants were loaded into a 15 % SDS polyacrylamide gel and stained by Coomassie Brilliant Blue.

The large scale production and purification of the H97D AfArsR protein was performed in the same way as the wild type AfArsR.

Protein concentration determination

Since the AfArsR protein sequence contains no tryptophans and bears only three tyrosines, the sequence based concentration determination, using absorbance values recorded at 280 nm, turned out to be unreliable, similarly to what we experienced with another metalloregulatory protein CueR, also displaying small number of these residues.[6] Other assays could not be implemented because of the presence of a reducing agent in the protein solution. Therefore, we have developed a reverse phase HPLC based amino acid separation and concentration determination protocol with a low-infrastructure demand, using a Shimadzu LC-20 instrument, equipped with a Phenomenex Synergi 4u Fusion-RP 80A C18 (150x4.6 mm, 4 µm) column. First we have tested the separation of amino acids by using an amino acid mixture, simulating the amino acid composition of the sequence of AfArsR. Since our simplistic protocol does not involve a derivatization step, most of the amino acids were eluted with low retention times. Nevertheless, chromatographic peaks of tyrosine, and especially, phenylalanine were well separated from each other and from all other amino acids of the mixture using an isocratic elution by 99 % – 1 % (*V*/*V*) water – acetonitrile, containing 0.1 % (*V*/*V*) PFPA (perfluoropentanoic acid) as an ion-pairing agent. Freshly prepared protein stock solutions were used for determining the accurate concentration of AfArsR, as well as the molar CD spectrum of the protein (see below in the "*Results and Discussion"* part, Fig. S1). After recording the CD spectra of the appropriately diluted fraction of the protein stock solution, a measured volume of the remaining stock was treated by 6 M HCl solution under vacuum at 110 °C for 24 hours. After completing the digestion of the protein, the sample was evaporated to dryness at 60 °C with an intense stream of argon. The hydrolysed products, deposited on the walls of the reaction vessels, were washed out quantitatively by the eluent (99.0%–0.9% H_2O–ACN + 0.1% PFPA) to be used during the chromatographic separation. A concentration series was prepared from a commercial phenylalanine product, covering the range where the concentration of phenylalanine in the hydrolysed sample was expected. A series of chromatograms, as calibration points, were recorded by injecting identical volumes from the elements of the phenylalanine standard series. Parallel injections from the hydrolysed samples and analysis of the phenylalanine peaks allowed us to determine the phenylalanine content of the protein, and accordingly, the exact concentration of AfArsR in the original stock solution. The whole procedure was executed twice with two separate AfArsR stock solutions. Based on the obtained concentration data and the recorded CD spectra, the molar CD spectrum of the protein was calculated, which was used afterwards for the convenient determination of the precise concentration of AfArsR solutions, using a small amount of the protein.

UV absorbance titrations

UV absorption titrations were carried out at 298 K on a Thermo Scientific Evolution 220 spectrophotometer using a 1.00 cm path length semi micro quartz cell (Hellma) equipped with a Teflon cap. Spectra were recorded in the wavelength range of 200 – 400 nm with 1 nm steps, applying a 0.25 s integration time at each point (corresponding to a ca.240 nm/min scan speed). Typical concentration of AfArsR in the titrated samples was 40 µM for protein monomer. Calculated volumes of the protein stock solution, containing ca. 0.4 mM TCEP as a reducing agent (see the "*Protein expression and purification*" section under the Materials chapter), were diluted into 10 mM phosphate buffer (pH = 7.5) to achieve the desired protein concentration in the titrated samples.

Aliquots of As^{III}, Sb^{III}, Hg^{II}, Cd^{II}, Zn^{II} and Pb^{II} solutions (whose concentrations were determined by complexometric titrations or based on precise weighing of the relevant stoichiometric salt, as described above in the "*Materials*" section) were pipetted into these samples and gently mixed, using automatic pipettes. Spectra were recorded from 0 equiv. up to a maximum of 10 equiv. of metalloids or metal ions per AfArsR dimer, depending on the studied system, after a sufficient equilibration time. 2-4 parallel experiments were carried out for all studied systems each containing typically 13-18 recorded spectra.

The obtained absorbance data were background corrected using a spectrum of a phosphate buffer solution having identical composition (including the ammonium-hydrogen carbonate and TCEP contents, originated from the protein stock) to those of the titrated samples. The background corrected data sets were used further for calculating stability data for the binding of the metalloids to AfArsR. For demonstration purposes, the background corrected spectra were normalized to an identical c = 40.0 µM protein concentration for easier comparability and for easier observation of the trends in absorbance changes. The errors of the absorbances of samples from the parallel experiments with various (semi)metal ion / protein dimer ratios were calculated as standard deviation values (s) using the regular formula for each sample:

$$s = \sqrt{\frac{\sum_{i=1}^{n}(x_i - \bar{x})^2}{n-1}}$$

Circular dichroism (CD) spectroscopy

CD spectra were measured with a JASCO J-1500 CD spectrometer in a continuous mode, using the wavelength range of 185 – 330 nm with a 20 nm/min scan speed. Data points were recorded with 1 nm steps, using 2 s D.I.T. and 200 mdeg/1.0 dOD CD scale and 2 scans were accumulated for each sample filled into a cylindrical cuvette of 0.2 mm pathlength. The samples contained the AfArsR protein at 20 – 30 µM final monomer concentration diluted by filtered MilliQ water. For background correction, a background sample was prepared by an identical dilution of the filtrate of the last cycle in the the final buffer exchange procedure in the purification process of the protein. The calculation of the $\Delta\varepsilon$ spectrum of the AfArsR protein is based on the following equation:

$$\Delta\varepsilon = \frac{CD\ (mdeg)}{32980 \times c_{monomer}(M) \times l\ (cm)}$$

where *CD* is the recorded CD intensities in millidegrees, $c_{monomer}$ is the actual concentration of the AfArsR monomers in mol/dm^3 unit, *l* is the used pathlength in centimetres. The accepted molar spectrum was calculated from two parallel experiments and the exact concentration of the samples was determined as described above in section *"Protein concentration determination"*. The concentration of protein stock solutions were calculated by recording CD spectra of their diluted samples and applying the molar CD spectrum and the pathlength of the cell, according to the Lambert-Beer law.

Mass spectrometry analysis

Mass spectra were recorded on an Orbitrap Elite (Thermo Scientific) mass spectrometer coupled with a NanoMate TriVersa (Advion) chip-based nano-electrospray ion source, using a 1.3 – 1.4 keV capillary voltage and 300 °C for the source temperature. Data evaluation and deconvolution were carried out by the Xcalibur 2.2 (Thermo) software. Typical samples for recording the native mass spectra contained the AfArsR protein at 11 µM monomer concentration in an ammonium-bicarbonate buffer (pH=7.6, 10 mM). Arsenous acid, mercury(II) chloride or potassium antimonyl tartrate was added into the samples in concentrations indicated in the legends for the relevant figures, *vide infra*.

^{199m}Hg PAC spectroscopy

Isotope production

^{199m}Hg PAC studies were carried out at the ISOLDE facility at CERN.[7] The metastable ^{199m}Hg isotopes, as well as several other radionuclides, were produced by the irradiation of a liquid lead target with high energy protons, and a very pure beam of the desired ^{199m}Hg was provided by a general purpose separator (GPS). This pure beam was implanted into a small volume of frozen MilliQ water (140-175 µL) placed into in a Teflon cup on a copper base which was kept at low temperature throughout the irradiation via a cold finger, immersed into liquid nitrogen.

Preparation of samples for ^{199m}Hg PAC spectroscopy

$Hg(Cys)_2$ solid was prepared as a reference compound according to the previously described procedure.[8] Sample preparations lasted for ca. 15-30 min allowing sufficient time for equilibration in the final samples containing all components. The irradiated ice disk, containing ^{199m}Hg, was thawed on a carefully heated copper plate and the liquid was transferred into a sample tube used for the experiments. As a first step, it was mixed with 5-40 µL non-radioactive $HgCl_2$ solution of appropriate concentration to achieve the desired concentration of Hg^{II} in the final sample. To this sample, 40 µL of the protein stock solution, prepared in 20 mM NH_4HCO_3 with 0.4 mM TCEP, was added. 10 µL of a buffer solution (*c* = 0.5 M – phosphate, MES or CHES buffer) was mixed into the samples. Na_2HPO_4/NaH_2PO_4 buffer was used for samples at pH ~ 7.4, while samples at pH ~ 6.2 and 9.0 were prepared by using MES and CHES buffers, respectively. The final pH values were adjusted by 1.0/0.1 M NaOH and/or $HClO_4$ solutions. Finally, sucrose (50 % *w/w*) was added to the samples and dissolved by using a Vortex mixer. The pH values were measured before the experiments at room temperature and recalculated to the temperature of the experiments executed at 1 °C by the temperature dependence of the different buffers.[9] It means that as a first step, the ratio of the two components of the conjugate acid-base pair of the applied buffer, corresponding to the desired pH value at 1 °C, was calculated by the known apparent pK_a value (at 1 °C) for this buffer system (i.e. 10 mM dihydrogen phosphate/monohydrogen phosphate – pK_{app} = 7.07; 10 mM zwitterionic and negatively charged forms of 2-(N-morpholino)ethanesulfonic acid (MES) – pK_{app} = 6.44; 10 mM zwitterionic and negatively charged forms 2-(Cyclohexylamino)ethanesulfonic acid (CHES) – pK_{app} = 9.82). Then the pH value for the measured sample to be set at 25 °C was calculated according to the apparent pK_a value for 25 °C (i.e. 10 mM dihydrogen phosphate/monohydrogen phosphate – pK_{app} = 7.00; 10 mM zwitterionic and negatively charged forms of 2-(N-morpholino)ethanesulfonic acid (MES) – pK_{app} = 6.17; 10 mM zwitterionic and negatively charged forms 2-(Cyclohexylamino)ethanesulfonic acid (CHES) – pK_{app} = 9.38). After the experiments and the decay of radioactive mercury, the pH values were verified. The concentration of the AfArsR protein in the final samples was 3.3×10^{-6} M protein dimer. The Hg^{II}:$AfArsR_{dim}$ concentration ratio was 0.5:1 for the pH-series and varied from 0.5:1 to 3.8:1 in the Hg^{II}-concentration series, carried at a constant pH (=7.4).

PAC instruments and data analysis

A digital PAC setup was used (DIGIPAC[10]) equipped with six 1.5”x1.5” $LaBr_3$(Ce) detectors. The time resolution was 0.6 ns and the time-per-channel calibrations was 0.04883 ns. Data analysis was carried out with the Winfit program (provided by prof. T. Butz) using 350 data points (excluding the first 10 points due to systematic errors in these). A Lorentzian line shape was used to account for line broadening, given by the parameter δ, due to a static distribution of EFGs. Fourier transformation of the data and fits were carried out using 350 points and a Keiser-Bessel function with the window parameter equal to 4. All spectra could not be analysed with a single NQI, so an initial guess of two NQIs was established by fitting to the two extremes of the Hg^{II} concentration series, i.e. the experiments with experimental conditions indicated in rows 1 and 3 of Table S3. All spectra were then analysed with these two NQIs as the initial guess of PAC parameters.

For ^{199m}Hg (intermediate nuclear level with *I* = 5/2), a time independent EFG, and randomly oriented molecules, the perturbation function is described by[11,12]:

$$A_{22}^{eff} G_{22}(t) = A_{22}^{eff} (a_0 + a_1 \cos(\omega_1 t) + a_2 \cos(\omega_2 t) + a_3 \cos(\omega_3 t))$$

where A_{22}^{eff} is the effective anisotropy, and a_i and ω_i depend on the quadrupole coupling constant ν_Q and the asymmetry parameter η of the NQI.[12] The experimental equivalent of $A_{22}^{eff}G_{22}(t)$ to which the NQI parameters are fitted is[12]:

$$R(t) = 2\frac{W(180°,t) - W(90°,t)}{W(180°,t) + 2W(90°,t)}$$

where *W(*180°*,t)* and *W(*90°*,t)* are the geometrical mean of coincidence spectra recorded with 180° and 90° between detectors.

Experimental procedures of Electrophoretic Mobility Shift Assays (EMSA)

The specific 38 basepair long double strand DNA (arsR DNA), including the sequence of the AfArsR recognition site, was obtained by the hybridization of the forward (5'- CATCCACGAATATTTCTTGCAGTATTGACAAGATATCG -3') and reverse (5'- CGATATCTTGTCAATACTGCAAGAAATATTCGTGGATG -3') oligonucleotides (Fasmac) by 1 °C/min cooling from 95 °C to 10 °C in 100 µM final concentration, in the presence of 10 mM $NaClO_4$. For some experiments, the previously described 42 bp long specific DNA (used for the pdUA-AfArsR plasmid construction, see above in section "*Plasmid constructions"*) was used, but no significant difference was observed in the data obtained with the 38 bp or 42 bp long DNA. A typical EMSA sample consisted of 1.55 µM arsR DNA, 10 % (*V*/*V*) glycerol and 10 mM phosphate buffer, pH = 7.5. The concentration of the protein dimer was gradually changed from 0 to 50 µM in experiments for investigating the stability of the protein–DNA complex. Concentration of the AfArsR was kept constant at 18.6 µM (for monomers) in the metal(loid) selectivity assays, while H97D mutant AfArsR was used at a monomer concentration of 24.8 µM. Preparation of the samples was according to the following protocol: AfArsR was first mixed with solutions of various metalloids or metal ions at the desired M^{III}/M^{II} to AfArsR dimer concentration ratio. This mixture was incubated at room temperature for 30 minutes, except for the Pb^{II} containing samples, where the waiting time was around 1.5 hours, because of the slow kinetics observed during the UV absorbance titration experiments. Solutions of the specific DNA was added to the metal ion-free protein solutions or to the mixtures of AfArsR and the metalloids/metal ions and then incubated at room temperature for another 20 minutes. For the metal ion competition experiments, the protein solution was first incubated with solutions of As^{III} or Sb^{III} applying a 2:1 metalloid per protein dimer concentration ratio (30 min), followed by the incubation of this mixture with the DNA (20 min). Finally, a small volume from the solution of the competitor metal ion was added to the sample using identical concentration to that of the metalloid. The final sample was incubated for an additional 30 minutes (or 1.5 hours with Pb^{II}). In experiments studying the effect of DMSA, this chelator ligand was also added in the final step, i.e. together with the competing Hg^{II} ions in samples containing both As^{III} and Hg^{II}.

2.5 µL fractions of these reaction mixtures (containing ca. 100 ng DNA) were loaded into a 6% (*m*/*V*) native polyacrylamide gel. A vertical electrophoresis at 100 V (Mini-PROTEAN Tetra Cell) was carried out using a running buffer of 12.5 mM TRIS and 96 mM glycine at 4 °C for 25 minutes. 5 µl FastRuler Ultra Low Range DNA Ladder (Thermo Scientific) was used as a reference. DNA probes were visualized by 0.5 µg/ml EtBr staining for 15 minutes using an Uvitec BTS 20MS gel documentation system. The intensities of the DNA bands on the electropherograms were analysed and manually integrated by the ImageJ softver.[13]

Intracellular I-Block assays

The intracellular I-Block assay[14] is based on the measurement of the β-galactosidase activity either by checking the colour of the bacterial colonies on an Luria agar plate containing X-gal (5-bromo-4-chloro-3-indolyl-β-D-galactopyranoside) substrate yielding blue colour upon cleavage by the β-galactosidase enzyme or by following the absorbance of the *o*-nitrophenol at 420 nm produced from the ONPG (ortho-nitrophenyl-β-galactoside) substrate. The expression of this enzyme is blocked by the LacI protein. This inhibitory protein is expressed from the pdUA-$LacI_{NE}$ vector, therefore by inserting the specific recognition DNA fragment of our protein of interest (AfArsR) upstream of the lacI gene in the pdUA-$LacI_{NE}$ plasmid (described above in the "*Plasmid construction*" section) the expression of the LacI inhibitor can be regulated upon AfArsR interaction by its DNA recognition site. The appropriate ER1821ΔlacI cells established for the I-Block experiments were kindly provided by Dr. Antal

Kiss.[14] During the transformation process, ~100 ng plasmid DNA was mixed with 20-50 µl of the ER1821ΔlacI competent cells and placed on ice for 30 minutes. This mixture was then incubated at 42 °C for two minutes then put back on ice for five more minutes. This suspension was mixed with 40-100 µl antibiotic-free LB medium and was incubated for 30 minutes at 37 °C with 150 rpm shaking. In the following step, the mixture was plated on antibiotic containing LB-agar Petri-dishes, which were then incubated overnight at 37 °C. We used ampicillin at 0.1 mg/ml concentration for the cells transformed by a pBAD plasmid and 0.05 mg/ml kanamycin for cells carrying a pdUA plasmid and both for the double transformation. Colonies were grown only if the transformation was successful. A single colony was transferred into 5 ml LB medium containing the appropriate antibiotics, and was incubated at 37 °C with 180 rpm shaking until OD_{600} reached 1. The transformed and grown cells were stored in 20 % (v/v) glycerol at –80 °C and 5-10 µL of these stocks were taken out to inoculate a new portion of LB media for follow up experiments.

In the experiments with X-gal, separate batches of Luria agar (LA) plates were prepared containing 40 µg/mL X-gal, and combinations of the following supplements according to Table S2: 50 µg/mL kanamycin, 100 µg/mL ampicillin, 1.2 mM glucose, and 0.6 mM arabinose, as well as metal(loid) solutions to yield a final concentration of 20 µM As^{III}, 1 µM Hg^{II}, or 20 µM Zn^{II}. The control medium did not contain heavy metal(loid)s. Approximately 20 mL of each of the medium was immediately poured into sterile Petri dishes and allowed to solidify. The doubly transformed bacteria with pdUA and pBAD plasmids were retrieved from the glycerol containing stocks stored at –80 °C. Cells were transferred into a 200 µL aliquots of Luria-Bertani (LB) broth using a sterile toothpick. The culture was then incubated at 37 °C with shaking (400 rpm) for 40 minutes. For plating, 40 µL aliqouts of the culture were spread evenly onto the surface. All plates were incubated at 37 °C for 16 hours and the colour of the colonies was checked visually.

Table S2 Concentration of components added to the Luria agar plates (P1-4) to adjust the appropriate conditions for the I-Block experiments.

	P1	P2	P3	P4
Kanamycin	50 µg/mL			
Ampicillin	100 µg/mL			
X-gal	40 µg/mL			
Glucose	1.2 mM			
Arabinose	0.6 mM			
As^{III}	-	20 µM	-	-
Hg^{II}	-	-	1 µM *	-
Zn^{II}	-	-	-	20 µM

* Experiments using a 20 µM Hg^{II} proved to be toxic to most of the cells, thus reduced concentration was applied

Experiments with ONPG were performed in 96 well PS F-bottom clear microplates (Iwaki) similarly to our previous work.[15] ER1821ΔlacI cells containing the pdUA-$lacI_{NE}$-AfArsR and/or the pBAD-AfArsR plasmids were pre-grown in LB media with the appropriate antibiotic(s) at 37 °C with 180 rpm shaking in test tubes. When OD_{600} ~ 0.3 was reached, 10-10 µl of the cell suspensions was transferred into a microplate with 300-300 µl LB media containing the antibiotic(s) and 20 mM L-arabinose to induce the expression of the AfArsR protein. The microplates were then incubated for 4 hours at 30 °C with 200 rpm shaking, when 5-5 µL arsenous acid, potassium antimonyl(III) tartrate, mercury(II) chloride, lead(II) chloride, cadmium(II) perchlorate and/or zinc(II) perchlorate solution was added into the appropriate wells at the indicated concentrations and the incubation was continued for 4 hours (8 hours incubation in total). Afterwards, we recorded the OD_{600} value of the samples in the wells by an Infinite M1000 Pro(Tecan) microplate reader, then 10 µl of the cultures were transferred into another 96 well microplate containing 45-45 µl cell membrane permeabilization solution (100 mM Na_2HPO_4, 2 mM $MgSO_4$, 20 mM KCl, 0.4 mg/ml sodium deoxycholate, 0.8 mg/ml CTAB and 5.4 µl/ml β-mercaptoethanol).

This microplate was incubated at 30 °C for 30 minutes with 200 rpm shaking, which was followed by the addition of 300-300 µl substrate solution (1 mg/ml ONPG, 40 mM NaH_2PO_4, 60 mM Na_2HPO_4 and 2.7 µl/ml β-mercaptoethanol) into each well to monitor the β-galactosidase activity by recording the absorbance at 550 and 420 nm in every 5 minutes for one hour at 30 °C with 10 second-long 300 rpm double-orbital shaking before each measurement cycle using an Infinite M1000 Pro(Tecan) microplate reader.

The β-galactosidase activity in Miller units was calculated via the following equation[14]:

$$\beta - galactosidase\ activity\ (\text{Miller unit}) = \frac{1000 \times \left(A_{420,60\ min} - A_{550,60\ min} \times F\right)}{60\ (min) \times V_{cell}(ml) \times OD_{600,cell}}$$

where $\boldsymbol{A_{420,60min}}$ and $\boldsymbol{A_{550,60min}}$ are the absorbances recorded after 60 minutes at 420 nm and 550 nm, respectively, corrected to 1 cm pathlength, ***F*** is a scalar for the baseline correction, $\boldsymbol{OD_{600,cell}}$ is the absorbance at 600 nm of the cell cultures in the wells after the 8 hour incubation of the first microplate, $\boldsymbol{V_{cell}}$ **(ml)** is the volume of these suspensions transferred to another plate containing the permeabilization solution. The F value was calculated for each sample via the following equation[15]:

$$F_{actual} = \frac{A_{420,t=0}}{A_{550,t=0}}$$

Since the absorbance values increase lineary with time up to 60 minutes, thus we used a linear fit of the data and calculated the absorbances at t = 0 and 60 minutes from the equation of the trendline.[15]

Based on our observations, repeating the experiments at different time points may result different absolute β-galactosidase activity values (Miller units), but the ratio of activities compared to the positive control cells (that contain only the gene of the ArsR protein) and negative control cells (that contain only the DNA recognition site vector) were similar. Therefore, when possible, relative β-galactosidase activity values were determined for better accuracy and comparability based on the following equation:

$$\beta\ Gal_{Rel} = \frac{\sum_{j=1}^{m}\sum_{i=1}^{n}\frac{PD_{ij} - \overline{D}_j}{\overline{P}_j - \overline{D}_j}}{m \cdot n} \pm (\sigma_{Rel}) \qquad \text{Eq. S1.a}$$

$$\sigma_{Rel} = \frac{\sqrt{\sum_{j=1}^{m}\sum_{i=1}^{n}\frac{\left(\overline{P}_j - \overline{D}_j\right)^2 \cdot {\sigma_{\overline{D}_j}}^2 + \left(PD_{ij} - \overline{D}_j\right)^2 \cdot \left({\sigma_{\overline{P}_j}}^2 + {\sigma_{\overline{D}_j}}^2\right)}{\left(\overline{P}_j - \overline{D}_j\right)^4}}}{m \cdot n} \qquad \text{Eq. S1.b}$$

where $\beta\ Gal_{Rel}$ is the relative β-galactosidase activity, σ_{Rel} is the standard deviation of the relative β-galactosidase activity, PD_{ij} is the absolute β-galactosidase activity of the i^{th} investigated sample in the j^{th} plate, containing both the Protein gene and the DNA recognition site vector, $\overline{P}_j$ and $\overline{D}_j$ are the average absolute β-galactosidase activity values of the positive, and negative controls in the in the j^{th} plate respectively. $\sigma_{\overline{P}_j}$ and $\sigma_{\overline{D}_j}$ are the standard deviations corresponding to the $\overline{P}_j$ and $\overline{D}_j$ control β-galactosidase activity values, while n is the number of parallel samples in a single plate and m is the total number of repetition plates. Standard deviations of the average relative β-galactosidase activities, denoted by the vertical bars at the relevant columns, were calculated by a formula also taking into account error propagation.[16]

When the relative β-galactosidase activities of the metalloid/metal ion containing samples were compared to the samples of the same protein constructs in the absence of metalloid/metal ions, the fractional relative β-galactosidase activity values were calculated based on a modified equation:

$$\beta\ Gal_{Rel} = \frac{\sum_{j=1}^{m}\sum_{i=1}^{n}\frac{\frac{\left(PD_{ij}^{Metal}-\bar{D}_j\right)}{\left(\bar{P}_j-\bar{D}_j\right)}}{\sum_{i=1}^{n}\left(\frac{\left(\overline{PD}_j^{Metal\ free}-\bar{D}_j\right)}{\left(\bar{P}_j-\bar{D}_j\right)}\right)}}{m\cdot n} \pm (\sigma_{Rel}) \qquad \text{Eq. S2.a}$$

$$\sigma_{Rel} = \sqrt{\sum_{j=1}^{m}\sum_{i=1}^{n}\frac{\left(\frac{\sum_{i=1}^{n}\frac{\left(\overline{PD}_j^{Metal\ free}-\bar{D}_j\right)}{\left(\bar{P}_j-\bar{D}_j\right)}}{n}\right)^2\cdot\left(\frac{\left(\bar{P}_j-\bar{D}_j\right)^2\cdot\left(\sigma_{PD_{ij}^{Metal}}{}^2+\sigma_{\bar{D}_j}{}^2\right)+\left(PD_{ij}^{Metal}-\bar{D}_j\right)^2\cdot\left(\sigma_{\bar{P}_j}{}^2+\sigma_{\bar{D}_j}{}^2\right)}{\left(\bar{P}_j-\bar{D}_j\right)^4}\right)+\left(\frac{\left(PD_{ij}^{Metal}-\bar{D}_j\right)}{\left(\bar{P}_j-\bar{D}_j\right)}\right)^2\cdot\left(\frac{\sum_{i=1}^{n}\left(\frac{\left(\bar{P}_j-\bar{D}_j\right)^2\cdot\left(\sigma_{\overline{PD}_j^{Metal\ free}}{}^2+\sigma_{\bar{D}_j}{}^2\right)+\left(\overline{PD}_j^{Metal\ free}-\bar{D}_j\right)^2\cdot\left(\sigma_{\bar{P}_j}{}^2+\sigma_{\bar{D}_j}{}^2\right)}{\left(\bar{P}_j-\bar{D}_j\right)^4}\right)}{n^2}\right)}{\left(\frac{\sum_{i=1}^{n}\frac{\left(\overline{PD}_j^{Metal\ free}-\bar{D}_j\right)}{\left(\bar{P}_j-\bar{D}_j\right)}}{n}\right)^4}}}{m\cdot n} \qquad \text{Eq. S2.b}$$

which, in general, followed the same logic as the previous Eq. S1.a, but division by the relative β-galactosidase activity of the metal-free sample ($\overline{PD}_j^{Metal\ free}$) was also included.

Statistical analysis for demonstrating the significance of the obtained relative β-galactosidase activity data was carried out via two-sample t-tests. The calculations were performed by the Minitab software.[17] The results of statistical analysis are presented the "*High-throughput quantitative I-Block assays – Metalloid/metal ion dependence"* section.

Results and Discussion

Molar CD spectrum of the AfArsR protein

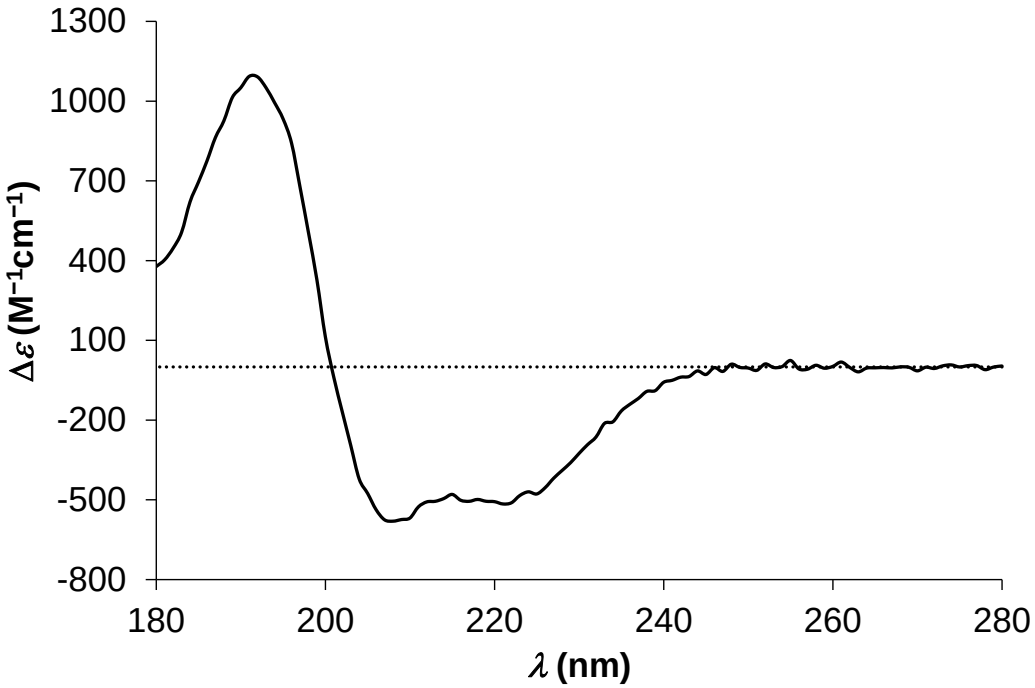

Fig. S1 Molar CD spectrum ($\Delta\varepsilon$) of the AfArsR protein.

UV absorbance titrations of the protein by Pb^{II}, Cd^{II} and Zn^{II}

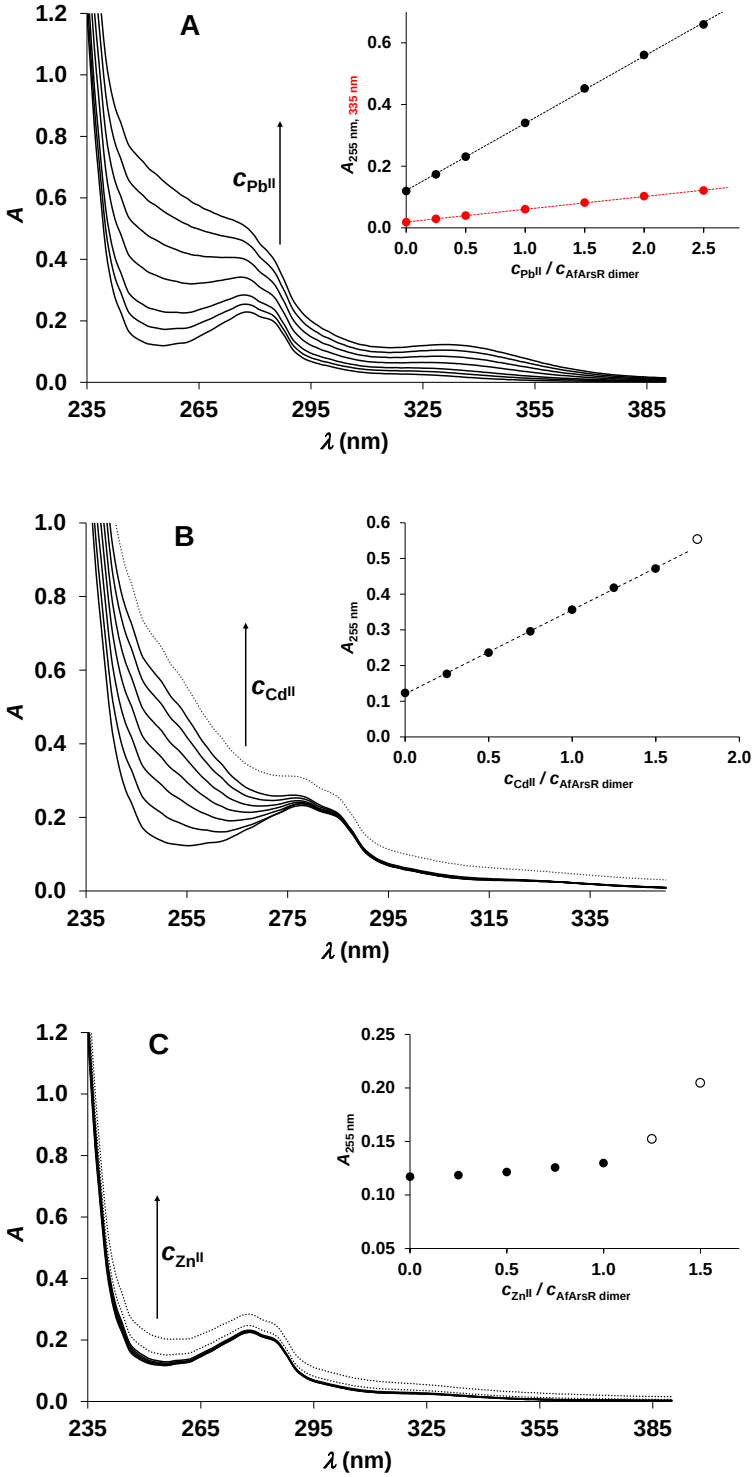

Fig. S2. UV-spectra recorded in the titration of AfArsR by solutions of Pb^{II} (A), Cd^{II} (B) and Zn^{II} (C). The arrows show the evolution of spectra along with the increasing metal ion concentrations, i.e. the increasing metal ion to protein concentration ratios. Spectra with dotted lines represent samples with indications of precipitate formation. In the insets, full circle symbols are absorbance traces at 255 nm (or 335 nm - Pb^{II}) while the dashed lines indicate the observed linear trends up to the point where precipitation occurs (these data points are depicted by empty circles). (c_{AfArsR} = 40.0 μM (for monomers) in 0.01 M phosphate buffer containing 120 μM TCEP).

ESI-MS data

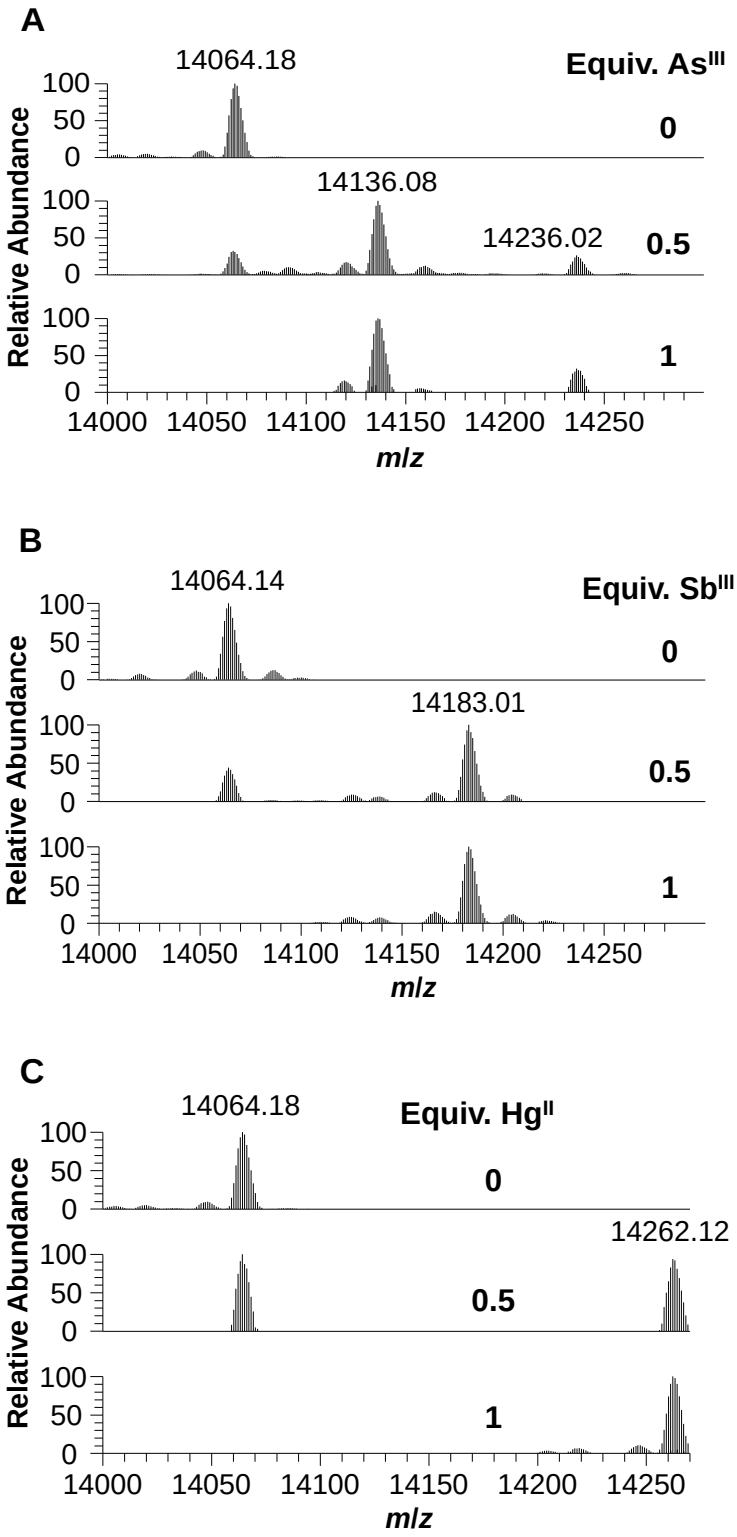

Fig. S3. Interaction of As^{III}, Sb^{III} and Hg^{II} with AfArsR, monitored by ESI mass spectrometry: deconvoluted native ESI-MS spectra of the protein with increasing concentrations of As^{III} (A), Sb^{III} (B) and Hg^{II} (C). c_{AfArsR} = 11 µM (for monomers), pH = 7.6 (10 mM NH_4HCO_3). Molar equivalents of metalloids and Hg^{II} are given per protein monomers. Note that under the conditions of ESI-MS only protein monomers, with or without the bound metalloids or metal ions, could be detected. These data indicate efficient binding of the metalloids and Hg^{II} to the AfArsR protein. Signals appearing around *m/z* = 14236 (panel A) are related to the formation of perchlorate adducts of the As^{III}-bound AfArsR (the source of the perchlorate ions is the arsenous acid stock solution – see the "*Materials"* section).

Evaluation of data from UV-titrations: speciation models and calculation of apparent stabilities for the As^{III} and Sb^{III} complexes

Data of the As^{III}/Sb^{III} titrations of the AfArsR protein (concentration series of the recorded UV absorption spectra) were evaluated using a ca. 90 nm wide spectral range (242 – 330 nm). The computer program PSEQUAD[18] was used for the fiting of data, allowing the calculation of stability constants ($\log\beta$ values) for the given species, according to the general equation below, representing apparent stabilities for the actual conditions (temperature (= 25 °C) , pH (= 7.5), buffer and salt contents of the samples):

$$\text{M + P} \rightleftharpoons \text{M-P} \qquad \log\beta = \log\frac{[\text{M-P}]}{[\text{M}]\cdot[\text{P}]}$$

In the above general equation, M denotes a metalloid and P stands for the protein (monomer or dimer, depending on the applied model – see below). Together with the $\log\beta$ values, the molar absorbance spectra of the absorbing complexes were also calculated, assuming the validity of the Lambert-Beer law and the additivity of the contribution of the individual absorbing species to the recorded absorbance values. Note that the molar absorbance values of the protein at each wavelength value (ε_λ, calculated, based on the known concentration of the AfArsR stock solution) were fixed in the fitting procedure.

Our first evaluation attempts involved the protein monomer ($AfArsR_{mon}$) and the metalloid (As^{III} or Sb^{III}) as the two basic components, as well as an M^{III}-$AfArsR_{mon}$ species (M^{III} is bound to the single metalation site of the protein monomer). However, these attempts resulted in unsatisfactory fits of the titration data, as shown in Fig. S4.

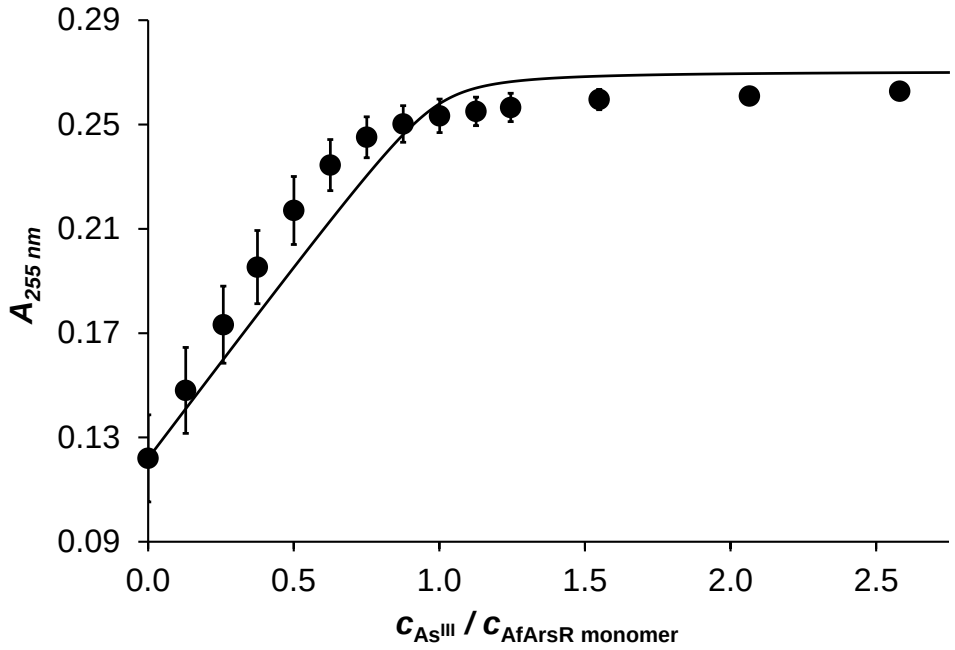

Fig. S4 Absorbance trace at 255 nm in the titration of AfArsR by a solution of As^{III} at pH = 7.5 (symbols represent averages of three independent experiments), fitted by a model involving AfArsR monomers and a single As^{III}-$AfArsR_{mon}$ species (c_{AfArsR} = 40.0 μM (for monomers)).

It was necessary to apply a sequential metalloid binding scheme, involving two metalloid binding events at the two sites of the AfArsR dimer ($AfArsR_{dim}$), to describe adequately the observed change in the As^{III}/Sb^{III} concentration dependent series of spectra. The protein dimer ($AfArsR_{dim}$) and the metalloid (As^{III} or Sb^{III}) were considered as the two basic components, and two complex species with their formation constants completed the model.

M^{III} + $AfArsR_{dim}$ ⇌ M^{III}-$AfArsR_{dim}$ $\quad \log\beta_1 = \log\frac{[M^{III}\text{-}AfArsR_{dim}]}{[M^{III}]\cdot[AfArsR_{dim}]}$

$2M^{III}$ + $AfArsR_{dim}$ ⇌ $(M^{III})_2$-$AfArsR_{dim}$ $\quad \log\beta_2 = \log\frac{[(M^{III})_2\text{-}AfArsR_{dim}]}{[M^{III}]^2\cdot[AfArsR_{dim}]}$

$\log\beta_1$ and $\log\beta_2$ values represent overall formation constants and one may easily derive association constants for the binding of the first and second metalloid to the AfArsR dimer from these data:

M^{III} + $AfArsR_{dim}$ ⇌ M^{III}-$AfArsR_{dim}$ $\quad \log K_1 = \log\beta_1$

M^{III} + M^{III}-$AfArsR_{dim}$ ⇌ $(M^{III})_2$-$AfArsR_{dim}$ $\quad \log K_2 = \log\beta_2 - \log\beta_1$

Since the binding of the first As^{III} or Sb^{III} turned out to be too strong, essentially stoichiometric and quantitative, it was necessary to fix $\log\beta_1$ to an estimated value. As described in the main part of the paper, we chose $\log\beta_1$ = 7.0 partially based on our own data and previously reported stability constants for As^{III}-multithiol complexes (see references in the manuscript). This stability is consistent with the quantitative binding of the first metalloid. We emphasize again that $\log\beta_1 = \log K_1 = 7.0$ used in the data fittings is only an estimate and this value can also moderately influence $\log\beta_2$, thus $\log K_2$. Accordingly, we have attempted fitting the data (both for As^{III} and Sb^{III}) by using different $\log\beta_1$ values. We allowed the program to optimize $\log\beta_2$ and the molar absorbance spectra of the two complexes freely, but the fitting parameter (an average of the differences between the measured and calculated absorbances) was found to be rather insensitive to the value of the fixed $\log\beta_1$. While using an estimate for $\log\beta_1$ = 5.5, the fitted value for the second As^{III}-binding step was $\log\beta_2$ = 9.6, and the fitting parameter increased by ca. 7 % (as compared to the model using $\log\beta_1$ = 7.0, see Fig. 2 in the main text). However, the first steep part of the absorbance trace profile (see Fig. S5) matches significantly less smoothly by the fitted curve, and this model produces unrealistic molar absorbance spectra, displaying a notably larger intensity for the As^{III}-$AfArsR_{dim}$ form, as compared to that of the $(As^{III})_2$-$AfArsR_{dim}$ complex.

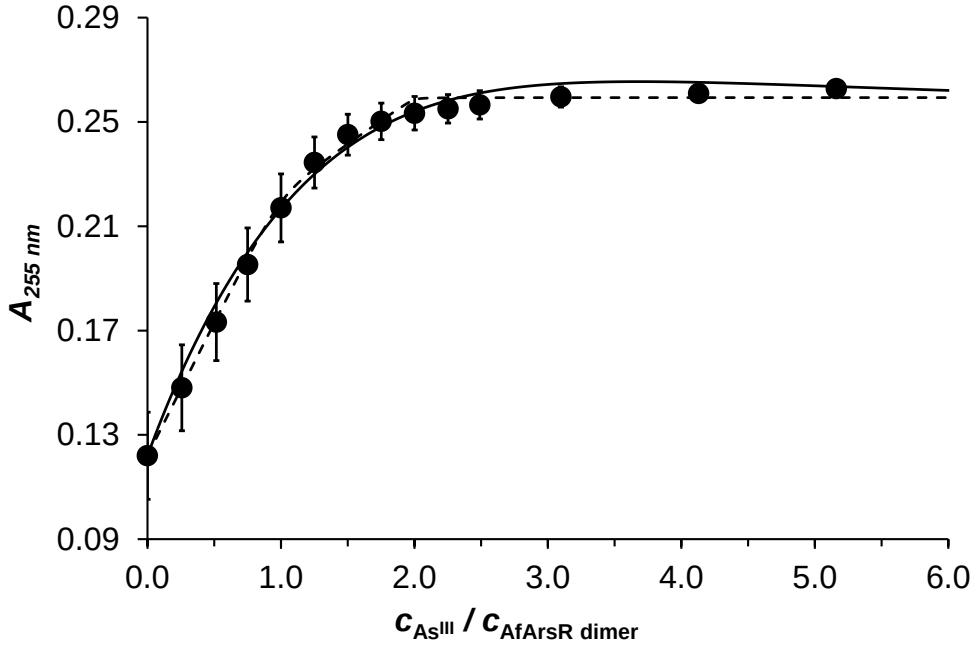

Fig. S5 Absorbance trace at 255 nm in the titration of AfArsR by a solution of As^{III} at pH = 7.5 (symbols represent averages of three independent series), fitted by a model involving AfArsR dimers and two consecutively formed complexes, As^{III}-$AfArsR_{dim}$ and $(As^{III})_2$-$AfArsR_{dim}$ (c_{AfArsR} = 40.0 μM (for monomers)). The dashed curve shows a fit carried out with $\log\beta_1$ (= $\log K_1$) fixed at 10.0 (resulting in $\log\beta_2$ = 17.92, i.e. $\lg K_2$ = 7.92) while the continuous line is a fit carried out with $\log\beta_1$ (= $\log K_1$) fixed at 5.0 (resulting in $\log\beta_2$ = 9.63, i.e. $\lg K_2$ = 4.63).

On the contrary, the increase of $\log\beta_1$ above 7.0 did not improve the fit of the data and the molar absorbance spectra of the two complexes (after subtracting the spectrum of the protein) change very little and reflect a ca. 30 % larger intensity for the $(As^{III})_2$-$AfArsR_{dim}$ complex compared to that of As^{III}-$AfArsR_{dim}$ species. Along with

with the further increase of $\log\beta_1$, the value of the $\log\beta_2$ value also increased, as well as the gap between the two constants, gradually converting the fitted curves into two phase curves (which is clearly not reflected by the measured data). The increasing difference between the two stability constants ($\log K_1$ and $\log K_2$) would suggest a larger negative cooperativity for the two binding events, albeit with a notably higher uncertainity affecting the stability constant for the second binding step. In sum, $\log\beta_1$ = 7.0 proved to be a reasonably good estimate that allows describing the sequential binding of As^{III} and Sb^{III} to the AfArsR protein.

It is worth noticing that the evaluated data of the As^{III} and Sb^{III} titration datasets reflect only a slightly higher binding affinity of the second Sb^{III} to the $AfArsR_{dim}$, relative to that of the second As^{III}: $\log K_2^{pH7.5}(As^{III})$ = 5.7, $\log K_2^{pH7.5}(Sb^{III})$ = 5.9. The relative affinities are, however, also influenced by the form of the two metalloids introduced into the studied samples. In contrast to As^{III} that was added as H_3AsO_3 from the As^{III} stock solution form, Sb^{III} was introduced in a form of its tartrate complex (see the *"Materials"* section) and thus the presence of a competing tartrate ligand also affects the conditional stability constants for the binding of Sb^{III}.

^{199m}Hg PAC data

Table S3. Fitted parameters for the recorded ^{199m}Hg PAC spectra with their errors in parentheses (last digit), see Fig. 4 and the discussion in the main text. The sample temperature was 1 °C and sucrose was added to 50 % (*w*/*w*) in all experiments, except the last entry. A note of "warning" related to the data analysis: each of the two NQIs display three peaks in the Fourier transformed data (because the ^{199m}Hg nuclei have I = 5/2 in the intermediate nuclear level). However, the position of the first (and most intense) of the three peaks are very similar for the two NQIs (see the red and blue indications in Fig. 4 in the main text). Thus, it can be difficult to reliably fit the parameters of the two NQIs. That is, it is possible that slightly different NQI combinations may give equally good fits. Qualitatively, the second peak of each NQI, appearing at ≈ 1.9 rad/ns (NQI1) and at ≈ 2.8 rad/ns (NQI2), allows for a better estimate of the relative amplitude of the two NQIs.

$AfArsR_{dim}$ (μM)	Hg^{II} (μM)	pH	ν_Q (GHz)	η	δ ×100	λ μs^{-1}	A ×100	χ_r^2
3.4	1.6	7.4	1.09(1) 1.52(6)	0.63(3) 0.28(15)	6(2) 0(7)	58(16)	11(1) 1(1)	0.72
3.4	8.1	7.4	1.06(3) 1.50(2)	0.63(6) 0.14(13)	11(4) 0(2)	28(14)	8(1) 3(1)	0.68
3.4	12.8	7.4	1.11(6) 1.48(2)	0.7(1) 0(1)	0(8) 4(2)	14(16)	1(1) 10(2)	0.77
3.4	1.6	6.2	1.14(2) 1.48(3)	0.72(4) 0(1)	0(2) 8(4)	24(15)	4(1) 10(3)	0.88
3.4 [a]	1.6	9.0	1.072(9) -	0.74(2) -	6(1) -	16(10)	11.6(7) -	0.66
Reference compound [b]			1.451(9)	0.06(7)		39(22)	15(1)	0.63

[a] The amplitude of the low frequency component was smaller than the error bar, and consequently the fit was conducted without this component.; [b] $Hg(Cys)_2$ solid reference.[8]

Results of Electrophoretic Mobility Shift Assays

Binding of the AfArsR dimer to the specific DNA

Interaction between the AfArsR protein and a specific DNA (38 or 42 bp, see the *"Experimental Procedures"* part) was followed by EMSA experiments using samples with increasing concentrations of the protein and a constant DNA concentration (1.55 μM) (Fig. S6). The derived fractions of the bound DNA, relative to the total DNA concentration at each point were calculated from the intensities of the relevant bands from the gels (*"Experimental procedures of Electrophoretic Mobility Shift Assays (EMSA)"*). These series of data points, as a function of the applied total concentrations of the protein and the DNA, were fitted by the computer program PSEQUAD.[18] In view of the dimerization constants published for the monomer-dimer protein equilibria of various ArsR-family member proteins ($\log K_{Dim}$ = 5.5 - SmtB from Synechococcus PCC7942),[19] $\log K_{Dim}$ = 7.0 - *Staphylococcus aureus* pI258 CadC,[20] $\log K_{Dim}$ = 5.2 - *Staphylococcus aureus* CzrA[21]), we expected that this equilibrium may operate in the studied system too, especially in the low AfArsR concentration regime that would affect the observed protein – DNA interaction. Lacking any independent data on the dimerization of AfArsR, we used the $\log K_D$ value for SmtB, the closest suggested analogue of AfArsR, and fixed this constant in our fitting procedure. This resulted in a modest, but notable (ca. 15 %) improvement in the fitting parameter and a small (~0.2 log units) change in the determined dimerization constant, too. The determined association constant for the

$$AfArsR_{dim} + DNA \rightleftharpoons AfArsR_{dim}{-}DNA$$

process, $\log K$ = 5.6(1) corresponding to a K_d = 2.5 μM value is close to what was reported previously for the interaction of AfArsR with a somewhat shorter, fluorophore labelled specific DNA (K_d = 0.9 μM).[22]

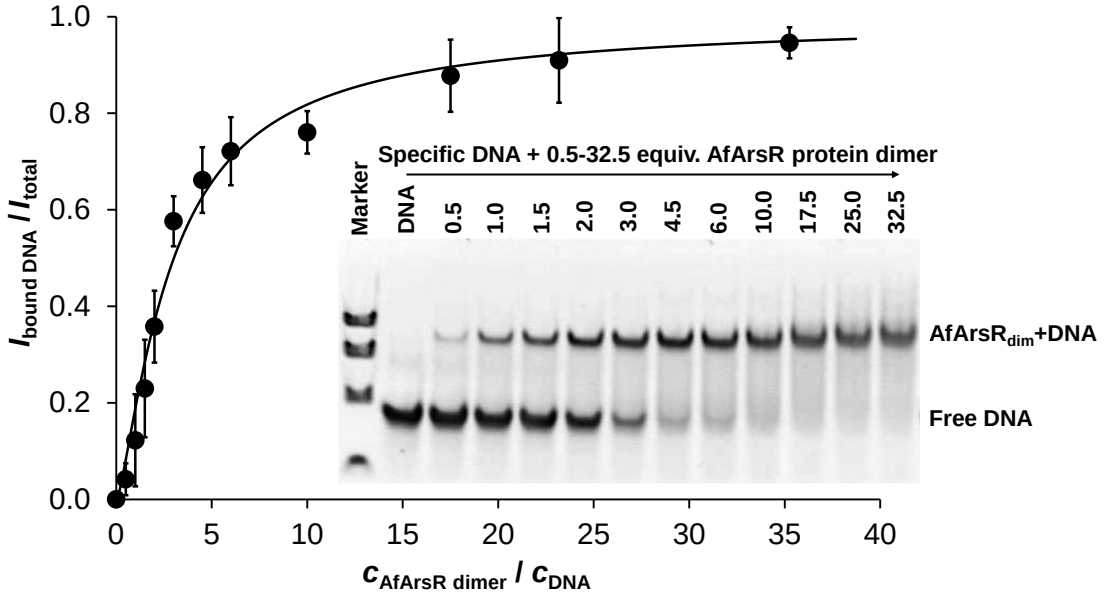

Fig. S6 Binding of the AfArsR dimer to a 42 bp specific DNA as a function of the AfArsR$_{dim}$:DNA concentration ratio, followed by EMSA. The intensity data used to derive the protein-bound and non-bound DNA fractions were obtained as described in the *"Experimental procedures of Electrophoretic Mobility Shift Assays (EMSA)"* section. The model used for the fitting involved the dimerization equilibrium of the AfArsR monomers with a fixed $\log K_{dim}$ value of 5.51, published for the suggested closest analogue[3] ArsR/SmtB family member SmtB protein (from *Synechococcus* PCC7942).[19] (pH = 7.5, c_{DNA} = 1.55 μM).

The effect of As^{III} on the DNA – H97D AfArsR complex

EMSA experiments were carried out with the H97D AfArsR mutant and followed the effect of As^{III} on the dissociation of the protein dimer from the DNA. Since our data indicated that a larger mutant protein excess, as compared to that of the wild type protein, is needed to achieve a similar ratio of the protein-bound and free DNA forms in the absence of As^{III}, we used an 8 : 1 H97D AfArsR dimer : DNA concentration ratio for the As^{III}-titration experiment (Fig. S7). (For the wild type protein, the protein dimer : DNA concetration ratio was 6 : 1, see the main text.) The As^{III}-dependence of the relative distribution of the free and protein-bound DNA indicates that the release of the H97D AfArsR from the DNA is completed between ca. 2.0-6.0-fold As^{III} excess relative to the concentration of the protein dimer, while ca. 1.5 equiv. As^{III} per protein dimer was enough to promote the complete dissociation of the wild type AfArsR (see Fig. 5A in the main text). This observation is in accord with findings of the I-Block assays suggesting that the H97D mutation has an influence on the metalloid response in the regulatory process governed by the AfArsR protein.

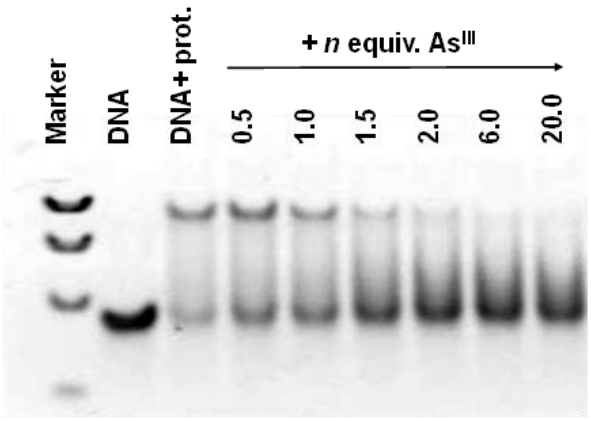

Fig. S7. Electrophoretic Mobility Shift Assay following the effect of increasing concentrations of As^{III} on the stability of the DNA-H97D $AfArsR_{dim}$ complex using c_{DNA} = 1.55 μM and $c_{H97D\ AfArsR\ monomer}$ = 24.8 μM corresponding to a 8 : 1 H97D AfArsR dimer : DNA concentration ratio

Results of I-Block experiments

Results of I-Block experiments on Luria agar plates

The I-Block experiments carried out on X-gal containing Luria agar plates P1-P4 (Table S2) clearly showed that binding of AfArsR to its target sequence inhibited the LacI protein expression and also reflected the different effects of the added metal(loid) compounds (Fig. S8). The cells grown on plate P1 in the absence of metal(loids) became blue due to the expression of the β-galactosidase and its ability to cleave the X-gal substrate. In contrast, the bacteria grown in the presence of As^{III} (P2) remained white, as a clear indication of the derepression process, i.e., the release of the DNA by AfArsR upon As^{III} binding. The selectivity of AfArsR against Hg^{II} and Zn^{II} divalent metal ions is demonstrated by the plates P3 and P4 where the cells turned into blue similarly to P1. This suggests that the eventual binding of these metal ions to AfArsR in cells could not promote the release of AfArsR from its target DNA sequence. These results supported the follow-up high-throughput experiments using a plate reader.

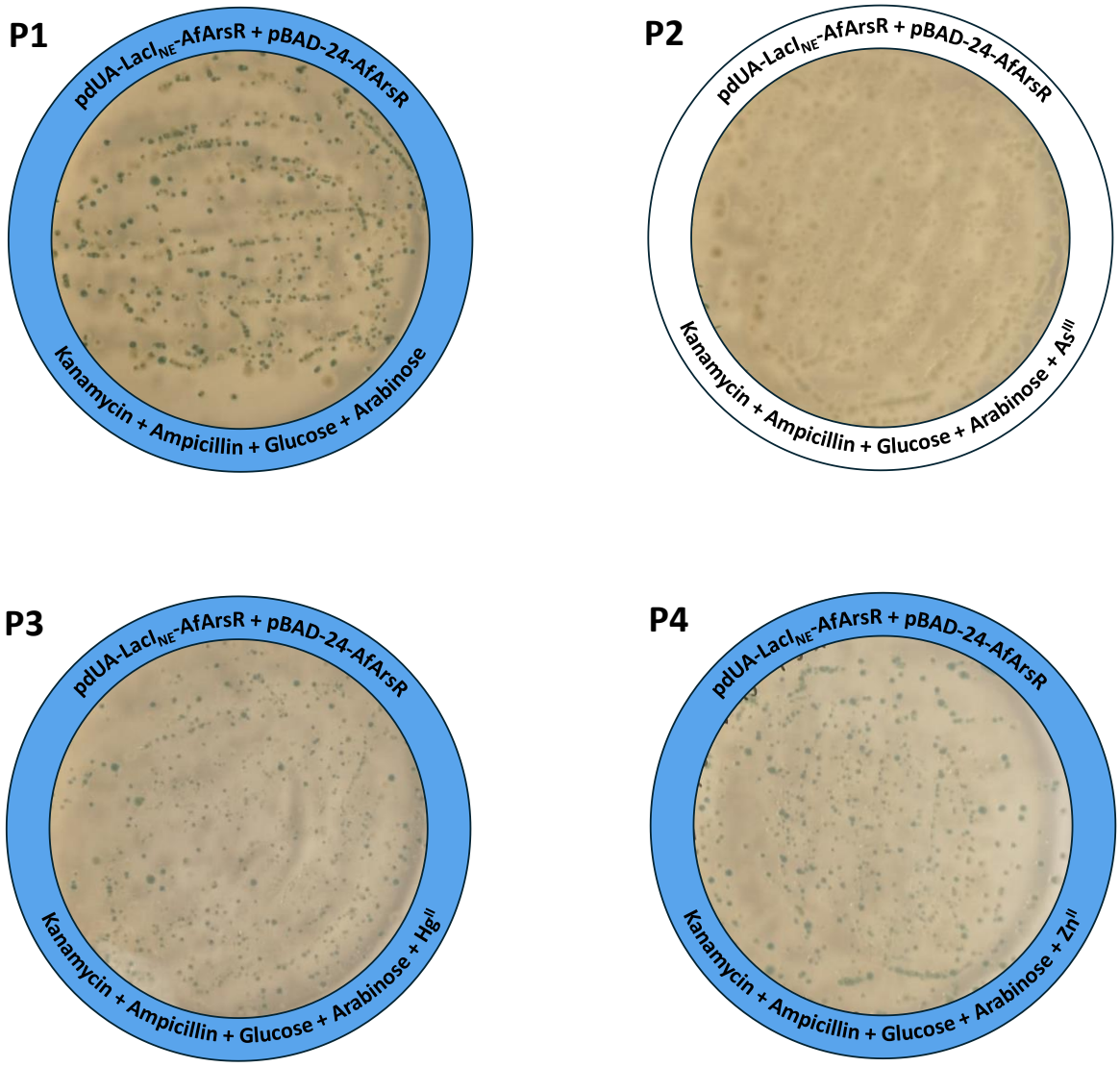

Fig. S8 I-Block experiments showing the effect of metal(loid) compounds on the bacterial cells grown on Luria agar plates containing supplements, as detailed in Table S2.

High-throughput quantitative I-Block assays – Metalloid/metal ion dependence

Relative β-galactosidase activities in our I-Block system were followed as a function of the As^{III} and Sb^{III} concentration. Fig. S9 shows that the metalloids are starting to influence the activities, as compared to the metalloid free sample, between 5 and 10 μM As^{III}/Sb^{III} and a maximal effect is reached at ca. 20 μM and 50 μM Sb^{III} and As^{III} concentration, respectively.

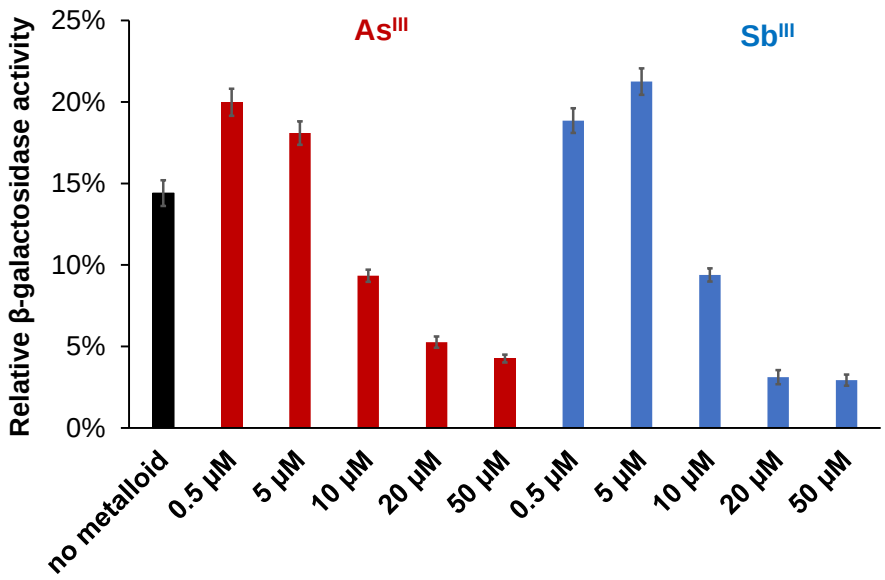

Fig. S9 The change of β-galactosidase activity in I-Block assays as an effect of the increasing concentration of As^{III} and Sb^{III} in the nutrient broth. The presented data are averages of 6-9 independent experiments. See the details of the experiments in section *"Intracellular I-Block assays"* in the *"Experimental Procedures"* part.

Two-sample t-tests were performed to investigte the significance of the relative β-galactosidase activities obtained for the different metal(loid) ion containing samples (Fig. 6 in the main text) and to demonstrate whether there is a significant difference relative to the activity of the the metal(loid) free sample at a $p = 0.05$ confidence level. Numbers in green-coloured cells in Table S4 reflect a significant drop of the relative β-galactosidase activities, while those in red-coloured cells indicate no significant difference in the presence of the studied metal ion.

Table S4. Statistical analysis of the effect of metal(loid) ions on the relative β-galactosidase activities presented in Fig. 6 in the main text using two-sample t-test at a $p = 0.05$ confidence level. The calculations were carried out by the Minitab program.[17]

Significance of the decrease of the relative β-Galactosidase activities in the presence of the metal(loid) ions												
As^{III}	Sb^{III}	Hg^{II}	Pb^{II}	Cd^{II}	Zn^{II}	As^{III} Hg^{II}	As^{III} Pb^{II}	As^{III} Cd^{II}	As^{III} Zn^{II}	Sb^{III} Pb^{II}	Sb^{III} Cd^{II}	Sb^{III} Zn^{II}
0.003	0.003	0.105	0.28	0.2	0.311	0.002	0.003	0.003	0.005	0.002	0.003	0.003

In order to verify that the relative β-galactosidase activities obtained in the AfArsR-based I-Block assays in the presence of the two metalloids (Fig. S9) or with different non-cognate metal ions (see Fig. 6 in the main text) are not notably impacted by the cytotoxic effects of the studied effectors, we examined the growth and viability of the bacterial cells. As an indicator of their potential toxic effects, we compared the OD_{600} values of the cell cultures, containing varying, but identical concentrations of the metalloids As^{III}/Sb^{III} (Fig. S10) and the divalent metal ions (Fig. S11), at the end of the 8-hour incubation at 30 °C. We added the metalloids/metal ions into the cell cultures after 4 hours of incubation, when the cells already reached OD_{600} = 0.2 – 0.3. but no significant effect of any of the studied effectors on the rate of the cell growth could be seen in the following 4 hours (within the applied concentration range), regardless of the plasmid content in the cells (Fig. S10 and Fig. S11). Therefore, it is reasonable to claim that the observed decrease of the β-galactosidase activities upon addition of the metalloids to the I-Block systems are not attributed to the toxicity of As^{III} or Sb^{III}, and the lack of notable derepression by divalent metal ions is not related to a toxic effect either.

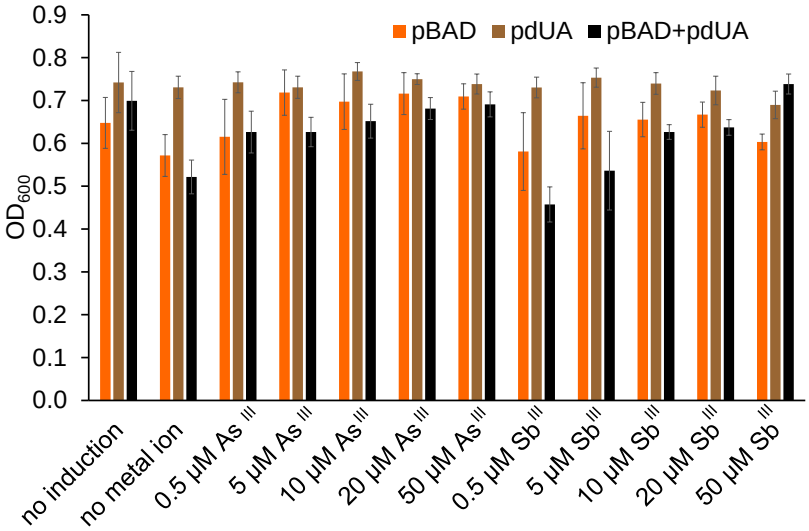

Fig. S10 OD_{600} values of the I-Block cells (ER1821ΔlacI cells transformed by the plasmids pBAD/myc-His-C containing the AfArsR gene (pBAD, orange) or by pdUA-$lacI_{NE}$ containing the recognition site of the AfArsR protein (pdUA, brown) or by both types of the previous plasmids (pBAD+pdUA, black)) at the end of the 8 hour-long incubation at 30 °C with 20 mM L-arabinose in the presence of the the indicated concentrations of metalloids (added to the cell cultures after 4 h incubation).

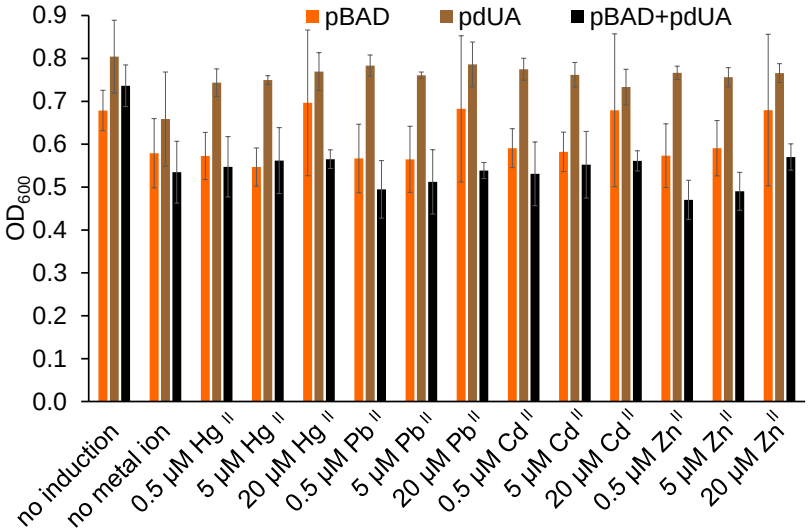

Fig. S11 OD_{600} values of the I-Block cells (ER1821ΔlacI cells transformed by the plasmids pBAD/myc-His-C containing the AfArsR gene (pBAD, orange) or by pdUA-$lacI_{NE}$ containing the recognition site of the AfArsR protein (pdUA, brown) or by both types of the previous plasmids (pBAD+pdUA, black)) at the end of the 8 hour-long incubation at 30 °C with 20 mM L-arabinose in the presence of the indicated concentrations of divalent metal ions (added to the cell cultures after 4 h incubation).

High-throughput quantitative I-Block assays – Effect of selected point mutations near the metalloid binding site in the AfArsR protein

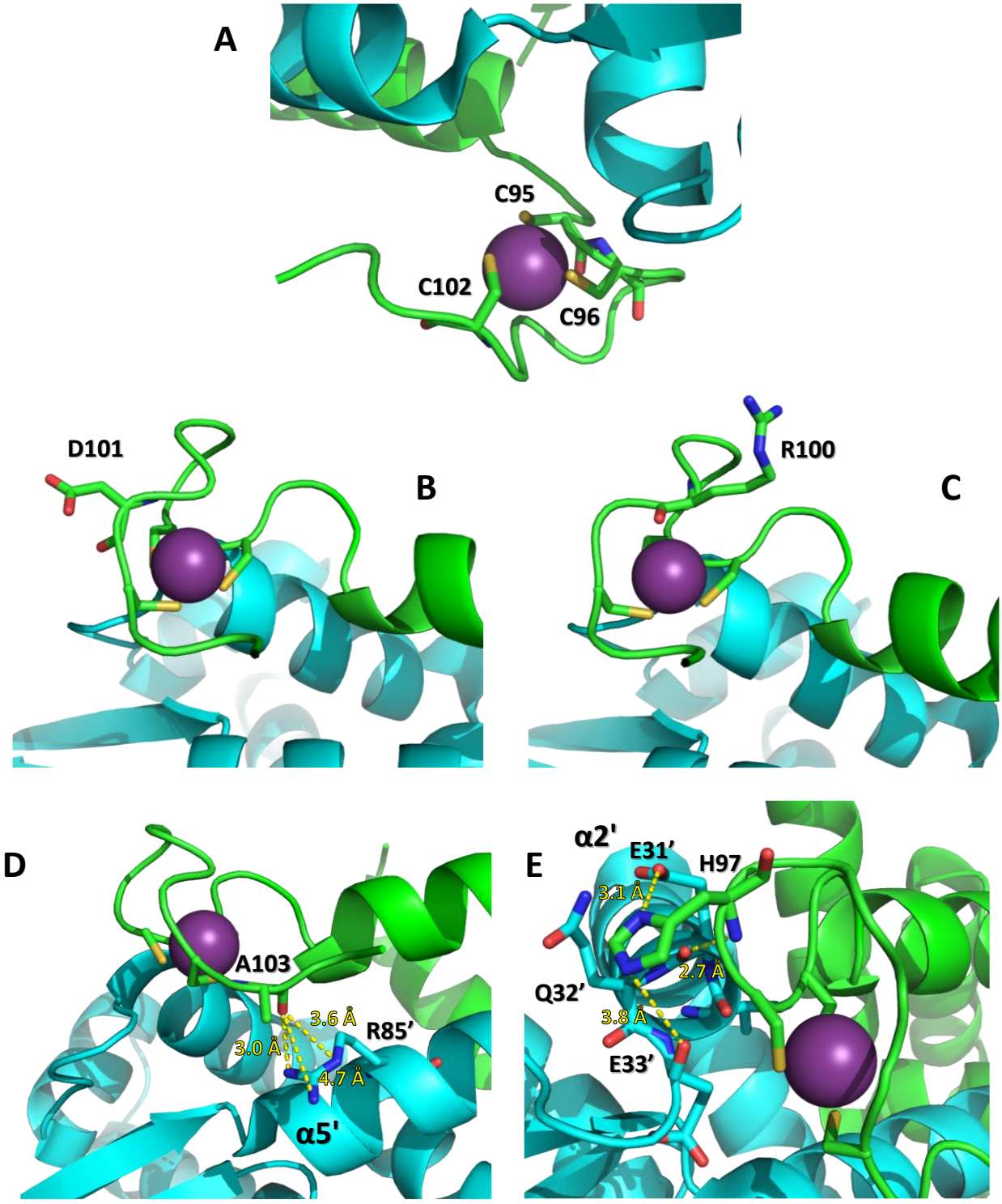

Fig. S12 Images of the As^{III}-binding site of the As^{III}-AfArsR structure (PDB: 6J05),[3] highlighting amino acid residues from the As-site, as well as plausible interactions between the metalloid binding site and nearby amino acid residues that may play a role in the metalloid selection and the allosteric mechanism of the derepression process. I-Block experiments were carried out with constructs, based on AfArsR variants displaying mutations at some of these amino acids. The mutated amino acids are as follows: the three coordinating Cys residues (A), the negatively charged Asp101 (B) and the positively charged Arg100 (C) from the metalloid binding segment, the potentially salt-bridging Arg85 from the α5' helix (D) and His97, the neighbour of the metalloid coordinating Cys96, forming possible links to the end of the α2' helix (E) of the other monomer, displaying negatively charged residues. See further discussion in the main text.

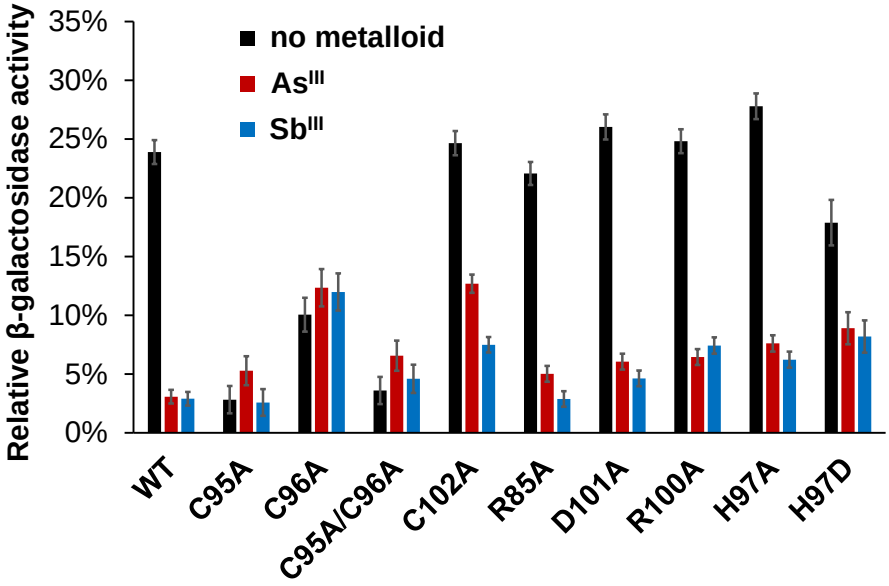

Fig. S13 The change of β-galactosidase activity in I-Block assays as an effect of As^{III} and Sb^{III} added to the nutrient broth in a concentration of 20 µM using the wild type AfArsR (WT) and various AfArsR mutants, as the signalling element of the bioreporter constructs inducing the protein expression by 20 mM L-arabinose.

Two-sample t-tests were performed to investigte the significance of the relative β-galactosidase activities obtained for the samples containing the different AfArsR variants (Fig. 7 in the main text and Fig. S13). Table S5 demonstrates whether there is a significant change of the relative β-galactosidase activities as compared to that of the wild type AfArsR containing construct at a $p = 0.05$ confidence level (see the black coloumns in Fig. S13). Numbers in green-coloured cells of Table S5 reflect a significant drop of activities, while those in red-coloured cells indicate no significant effect of the introduced mutations. These data support the suggestion that the H97D mutation decreases the DNA-binding ability of AfArsR.

Table S5. Statistical analysis of the impact of the mutations, introduced into AfArsR, on the relative β-galactosidase activities presented in Fig. S13 using two-sample t-test at a $p = 0.05$ confidence level. The calculations were carried out by the Minitab program.[17]

	Significance of the decrease of the relative β-galactosidase activities obtained for the AfArsR mutant constructs as compared to the activity of the wild type protein carrying construct								
	C95A	C96A	C95A/C96A	C102A	R85A	D101A	R100A	H97A	H97D
pBAf	< 0.001	< 0.001	< 0.001	0.643	0.263	0.784	0.683	0.943	0.004

Table S6 demonstrates whether there is a significant impact of As^{III} or Sb^{III} on the relative β-galactosidase activity for a given AfArsR variant at a $p = 0.05$ confidence level, as compared to the observed effect in the wild type AfArsR construct. (See the fractions of the relative activities, as an effect of the metalloids, in Fig. 7 in the main text or compare the relative height of the three columns in Fig. S13). Numbers in green-coloured cells reflect a significantly different fraction of the relative β-galactosidase activity, as compared to the level found for the wild type construct. The effects of As^{III} and Sb^{III} in the C102A and H97D mutant constructs are notably weaker, as compared to the wild type AfArsR construct, suggesting that the elimination of the third metalloid binding Cys ligand and certain mutations at the position of His97 has an impact on the metalloid regulation process.

Table S6. Statistical analysis of the effect of metalloids on the the relative β-galactosidase activities obtained for the different AfArsR mutant constructs, in comparison to the effect of metalloids on the activity in the wild type system (see Fig. 7 in the main text), executed by using two-sample t-tests at a $p = 0.05$ confidence level. The calculations were carried out by the Minitab program.[17]

	Significance of the change of the relative β-galactosidase activities promoted by the metalloids in the AfArsR mutant constructs, as compared to the effects of metalloids on the activity of the wild type construct					
	C102A	R85A	D101A	R100A	H97A	H97D
As^{III} pBAf	< 0.001	0.691	0.569	0.357	0.284	< 0.001
	C102A	R85A	D101A	R100A	H97A	H97D
Sb^{III} pBAf	0.035	0.919	0.774	0.041	0.388	0.015

To validate the comparibality of the relative β-galactosidase activities in the I-Block systems of the different AfArsR mutants (black cloumns in Fig. S13), we compared the protein expression levels of these mutants. The SDS polyacrylamide gel image (Fig. S14), prepared according to the "*Protein expression and purification"* section, reflects that there is no significant difference between the expressed protein levels in the wild type and in most of the mutant constructs (including the H97D variant). Although there is some variation in the amount of observable overexpression, i.e. the C95A, C96A and C95A/C96A variants are expressed somewhat less efficiently than the wild type and other mutants, which may actually improve the cell growth in these bacterial cultures (manifested in the larger OD_{600} values at the end of the incubation period, see Fig S15 below), even the weakest protein band reflects a huge excess of the AfArsR protein variants compared to the number of DNA recognition sites inside the cell (considering that pdUA is a low copy number plasmid). Thus, the slight differences in the protein overexpression are unlikely to affect the reliability of the relative β-galactosidase activity data recorded in the I-Block experiments. In support, previous EMSA and cellular assays showed also that mutations at the C95 and C96 residues significantly retard the DNA binding ability of the modified protein,[23] in line with our own results.

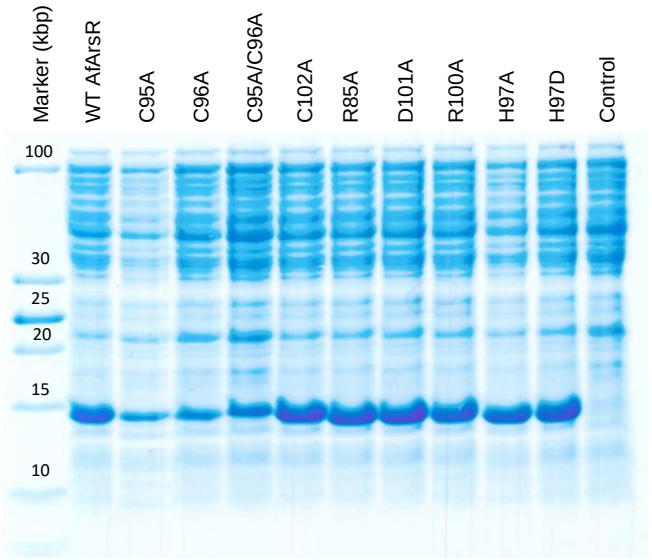

Fig. S14 SDS-PAGE image showing protein expression levels of the wild type and various mutant AfArsR proteins in BL21 (DE3) cells induced by 2.66 mM L-arabinose (except for the "Control" sample of the H97D mutant, where no arabinose was applied).

We have also verified the results of the I-Block assays using various AfArsR mutant constructs by monitoring whether the mutations have a significant effect on the rate of the cell growth. Fig. S15 shows that none of the studied mutations decreased the OD_{600} value compared to the wild type protein at the end of the incubation period, so they did not affect the cell growth through cytotoxic effects of the proteins. Even a bit larger OD_{600} values can be observed with the C95A, C96A and C95A/C96A variants, which probably goes hand in hand with the previously discussed phenomenom that they are expressed somewhat less efficiently, as mentioned above.

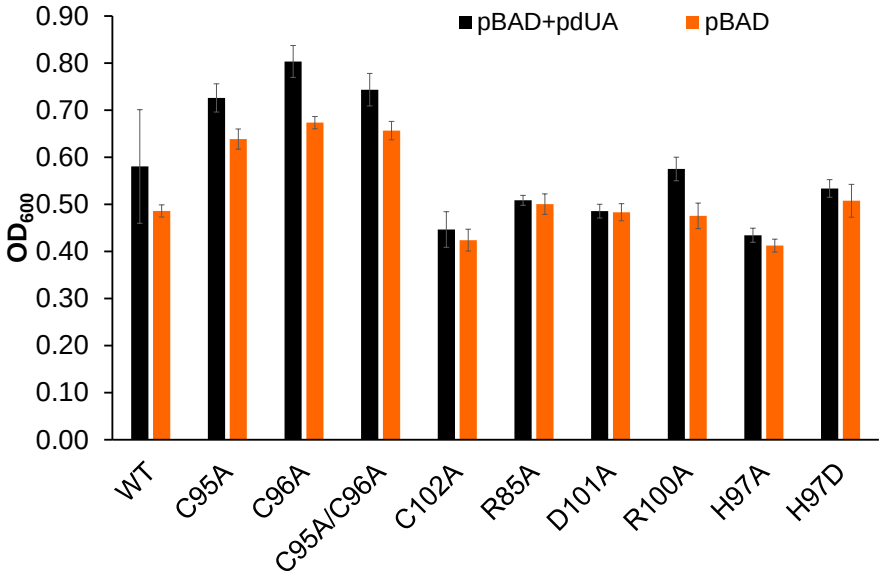

Fig. S15 OD_{600} values of the I-Block cells carrying the various AfArsR mutants (ER1821ΔlacI cells transformed by the pBAD/myc-His-C plasmid containing the AfArsR gene with the indicated mutations (pBAD, orange) or by the pBAD and a pdUA-$lacI_{NE}$ plasmid containing the recognition site of the AfArsR protein (pBAD+pdUA, black)) at the end of the 8 hour-long incubation at 30 °C with 20 mM L-arabinose.

References

1 A. Tóth, K. Sajdik, B. Gyurcsik, Z. H. Nafaee, E. Wéber, Z. Kele, N. J. Christensen, J. Schell, J. G. Correia, K. G. V. Sigfridsson Clauss, R. K. Pittkowski, P. W. Thulstrup, L. Hemmingsen, A. Jancsó, As^{III} selectively induces a disorder-to-order transition in the metalloid binding region of the AfArsR protein, *J. Am. Chem. Soc.*, 2024, **146**, 17009–17022.

2 R. Pribil, *Applied Complexometry*, ed. R.A. Chalmers, Pergamon Press, Oxford, UK, 1982.

3 C. Prabaharan, P. Kandavelu, C. Packianathan, B. P. Rosen, S. Thiyagarajan, Structures of two ArsR As(III)-responsive transcriptional repressors: Implications for the mechanism of derepression, *J. Struct. Biol*., 2019, **207**, 209–217.

4 L.-H. Chen, V. K. Köseoğlu, Z. T. Güvener, T. Myers-Morales, J. M. Reed, S. E. F. D'Orazio, K. W. Miller, M. Gomelsky, Cyclic di-GMP-dependent signaling pathways in the pathogenic firmicute *Listeria monocytogenes*, *PLoS Pathog.,* 2014, **10**, e1004301.

5 Z. H. Nafaee, É. Hunyadi-Gulyás, B. Gyurcsik, Temoneira-1 β-lactamase is not a metalloenzyme, but its native metal ion binding sites allow for purification by immobilized metal ion affinity chromatography, *Protein Expr Purif.*, 2023, **201**, 106169.

6 R. K. Balogh, E. Németh, N. C. Jones, S. V. Hoffmann, A. Jancsó, B. Gyurcsik, A study on the secondary structure of the metalloregulatory protein CueR: effect of pH, metal ions and DNA, *Eur. Biophys. J.*, 2021, **50**, 491–500.

7 R. Catherall, W. Andreazza, M. Breitenfeldt, A. Dorsival, G. J. Focker, T. P. Gharsa, T. J. Giles, J.-L. Grenard, F. Locci, P. Martins, S. Marzari, J. Schipper, A. Shornikov, T. Stora, The ISOLDE facility, *J. Phys. G: Nucl. Part. Phys.*, 2017, **44**, 094002.

8 A. Jancsó, J. G. Correia, R. K. Balogh, J. Schell, M. L. Jensen, D. Szunyogh, P. W. Thulstrup, L. Hemmingsen, A reference compound for ^{199m}Hg perturbed angular correlation of γ-rays spectroscopy, *Nucl. Instrum. Methods Phys. Res. A*, 2021, **1002**, 165154.

9 R. Beynon, J. Easterby, *Buffer Solutions*, Oxford University Press, New York, 1996.

10 M. Jäger, K. Iwig, T. Butz, A compact digital time differential perturbed angular correlation-spectrometer using field programmable gate arrays and various timestamp algorithms, *Rev. Sci. Instrum.*, 2011, **82**, 065105.

11 H. Frauenfelder, R. M. Steffen, In *Alpha-, Beta and Gamma-Ray Spectroscopy*, North Holland, Amsterdam, 1965, p. 997.

12 L. Hemmingsen, K. N. Sas, E. Danielsen, Biological applications of perturbed angular correlations of γ-ray spectroscopy, *Chem. Rev.*, 2004, **104**, 4027–4061.

13 C. A. Schneider, W. S. Rasband, K. W. Eliceiri, NIH Image to ImageJ: 25 years of image analysis, *Nat. Methods,* 2012, **9,** 671–675.

14 S. Szentes, N. Zsibrita, M. Koncz, E. Zsigmond, P. Salamon, Z. Pletl, A. Kiss, I-Block: a simple Escherichia coli-based assay for studying sequence-specific DNA binding of proteins, *Nucleic Acids Res.*, 2020, **48**, e28.

15 B. Hajdu, A. Tóth, B. Fazekas, M. Horvát, K. Kato, A. Kawaguchi, K. Nagata, A. Jancsó, B. Gyurcsik, DNA recognition, cleavage, and toxic metal ion interaction of an artificial zinc finger protein inside *E. coli* cells, *Prot. Sci*., 2026, (In production), DOI: 10.1002/pro.70599

16 H. Ku, Notes on the Use of Propagation of Error Formulas, *J. Res. Natl. Bur. Stand. C. Eng. Instrum.,* 1966, **70C**, 263–273.

17 A. Alin, Minitab, *WIREs Comp Stat*., 2010, **2**, 723–727.

18 L. Zékány, I. Nagypál, G. Peintler, *PSEQUAD for chemical equilibria*, Technical Software Distributors, Baltimore, MD, 1991.

19 S. R. Kar, A. C. Adams, J. Lebowitz, K. B. Taylor, L. M. Hall, The cyanobacterial repressor SmtB is predominantly a dimer and binds two Zn^{2+} ions per subunit, *Biochemistry*, 1997, **36**, 15343–15348.

20 L. S. Busenlehner, N. J. Cosper, R. A. Scott, B. P. Rosen, M. D. Wong, D. P. Giedroc, Spectroscopic properties of the metalloregulatory Cd(II) and Pb(II) sites of S. aureus pI258 CadC, *Biochemistry*, 2001, **40**, 4426–4436.

21 M. A. Pennella, J. E. Shokes, N. J. Cosper, R. A. Scott, D. P. Giedroc, Structural elements of metal selectivity in metal sensor proteins, *Proc. Natl. Acad. Sci. USA,* 2003, **100**, 3713–3718.

22 J. Chen, S. Sun, C.-Z. Li, Y.-G. Zhu, B.P. Rosen, Biosensor for organoarsenical herbicides and growth promoters, *Environ. Sci. Technol.,* 2014, **48**, 1141–1147.

23 J. Qin, H.-L. Fu, J. Ye, K. Z. Bencze, T. L. Stemmler, D. E. Rawlings, B. P. Rosen, Convergent evolution of a new arsenic binding site in the ArsR/SmtB family of metalloregulators, *J. Biol. Chem*., 2007, **282**, 34346–34355.